

Mineralogical and Genetical Study on Alabandite from the Manganese Deposits of Japan

Fukuoka, Masato
Faculty of Science, Kyushu University

<https://doi.org/10.5109/1546077>

出版情報 : 九州大学理学部紀要 : Series D, Geology. 24 (4), pp.207-251, 1981-12-25. Faculty of Science, Kyushu University

バージョン :

権利関係 :



Mineralogical and Genetical Study on Alabandite from the Manganese Deposits of Japan

Masato FUKUOKA

Abstract

The modes of occurrence, parageneses, and chemical composition of alabandite and associated minerals in sixty-three samples from nineteen manganese deposits in Japan are described on the basis of microscopic observation, X-ray powder diffraction, and electron probe microanalysis.

From the results obtained, the parageneses and chemical composition of alabandite are grouped into three types by the differences of the modes of occurrence. In the first type, alabandite occurs in coarse-grained rhodochrosite ore in Tertiary vein-type deposits with FeS content of 0.6 to 5.8 mol.%. In the second type, alabandite is dispersed in fine-grained rhodochrosite ore in unmetamorphosed bedded-type deposits with FeS range of 0.2 to 6.6 mol.%. In the third type, alabandite occurs abundantly in manganese silicates and oxides ore in thermally metamorphosed bedded-type deposits and has 0.3 to 13.5 mol.% FeS. The two bedded-type deposits were formed in Paleozoic to Mesozoic age.

In the second and third types, the FeS content in alabandite is closely correlated to the kinds of the associated minerals. Namely, the FeS content in alabandite associated with manganese oxides ore, tephroite ore, and rhodonite ore is less than 2 mol.%, 4 mol.%, and 13.5 mol.%, respectively. Especially in the third type, the above data indicate that FeS content of alabandite generally increases from the central to the peripheral parts of ore bodies.

This variation of the FeS content is explained not only by the differences in the distribution ratios of iron between alabandite and associated manganese oxides and silicates but also by the introduction of iron accompanied with sulfur into ore body during thermal metamorphism.

Moreover, considering the stability field of alabandite which was thermochemically calculated by using the selected principal reactions, it seems that alabandite could be frequently found in nature.

Content

	Page
I. Introduction	208
II. Previous studies	208
III. Locality and manganese deposits	210
IV. Experimental methods	211
V. Occurrence and paragenesis	213
VI. Compositional relation between alabandite and associated minerals	221
VII. Genetic environment of alabandite	232

VIII. Concluding remarks	235
Acknowledgements	236
References cited	237
Appendix	241

I. Introduction

Four synthetic phases of binary manganese-sulfur have been known. They are α -MnS (cubic, NaCl-type structure), β -MnS (cubic, sphalerite-type structure), β -MnS (hexagonal, wurtzite-type structure), and MnS₂ (cubic, pyrite-type structure) (WYCKOFF, 1921; SCHNAASE, 1933; MEHMED and HARALDSEN, 1938). Only α -MnS and MnS₂ are stable in nature and are called alabandite and hauerite, respectively. Hauerite has never been found in manganese deposits but occurs rarely in sulfur deposits, because it is stable under sulfur vapor pressures higher than approximately that compatible with the sulfur condensation curve (BILTZ and WIECHMANN, 1936; BARTON and SKINNER, 1979). Alabandite has been known to occur widely as a minor constituent in most manganese deposits in Japan, although it was formerly considered as an uncommon mineral.

Alabandite is now the common and the only mineral in the manganese-sulfur system in the manganese deposits. Therefore, it should be possible to use alabandite as an indicator of f_{s_2} (sulfur fugacity) which reflects the effect of the other predominant parameters (*e.g.*, temperature, f_{O_2} , f_{CO_2} , *etc.*) controlling mineral formation in the process of manganese ore formation. However, no genetical studies of natural alabandite have been conducted except for the brief reports of HEWETT and ROVE (1930), WATANABE (1939), and WATANABE and KIMURA (1954).

In this paper, a large number of alabandite samples from Paleozoic to Mesozoic bedded-type and Tertiary vein-type manganese deposits in Japan are described with respect to the mode of occurrence, chemical composition, and paragenetic relation in order to clarify the genetical environment of alabandite.

II. Previous studies

Some useful mineralogical works on natural or synthetic alabandite, especially made in Japan, are briefly reviewed.

A. Natural alabandite

Alabandite was first named by BEUDANT in 1832. In Japan, it was found for the first time from Ōishi mine, Akita Prefecture, by Tsunashirō WADA in 1916. Since then alabandite has been recognized and reported from about 60 manganese mines in Japan (Table 1).

WATANABE and KIMURA (1954) classified alabandite into two types on the basis of the mode of occurrence and paragenetic relation. One is epithermal deposit type, *i.e.*, the Tertiary rhodochrosite veins, in which alabandite is associated with euhedral or colloformal pyrite, marcasite, quartz, and rhodochrosite and occasionally with gold, silver, lead, or zinc bearing minerals. The other is

Table 1. List of alabandites reported from Japan.

Mine	Locality	Age*	Type	Associated Minerals**	Alabandite, FeS mol. % [†]	Notes on alabandite	References
Inakuraishi	Hokkaido	Miocene	Vein	<u>rhc</u> , mac, gn, sp, py, cp, tet, qz, pyr	4.7	0.01-1.5mm ^φ , irregular shape, dark green-dark greenish brown, rarely euhedral	1, 3, 25, 27, 36
Ōe	"	"	"	rhc, rhd, gn, sp, cp, py, tet, qz, pyr			22
Sankei	"	"	"	rhd, rhc, tet, cp, gn, sp, py, qz			36
Tamamori	"	"	"	rhc, gn, sp, py, cp, qz, tet		granular-prismatic aggregate	2
Yakumo	"	"	"	<u>rhc</u> , sp, gn, py, cp, tet, qz, pyr			34
Yūbaridake	"	Jurassic-Cretaceous	Bedded	<u>rhc</u> , <u>bar</u>	1.3	0.05mm ^φ , irregular grain, greenish black, opaque-nearly opaque	27
Ōishi	Akita	Miocene	Vein	<u>rhc</u>			11
Ōmori	"	"	"	<u>rhc</u>			11
Hijikuzu	Iwate	Jurassic	Bedded	<u>tep</u> , <u>rhd</u> , po, rhc, spt, bem, pw			20
Hongō	"	Permian	"	rhd, pxm, <u>tep</u> , spt, rhc, cp, py			21
Mitsune	"	Jurassic	"	rhd, <u>tep</u> , rhc		emulsion texture of pyrrhotite exsolution	18
Namiita	"	Permian	"	rhd, <u>tep</u>		"	18
Nodatamagawa	"	Permian-early Mesozoic	"	<u>rhc</u> , <u>tep</u> , rhd, hs, ms, gx, pw			24, 30, 31
Takamatsu	"	Traassic	"	rhd, <u>tep</u>		"	18
Taki	"	Jurassic	"	rhd, <u>tep</u> , rhc, hs, jb, spt, pw, gx			19
Mori	Yamagata	Miocene	Vein	<u>rhc</u> , qz, sp, gn, py, mac, bar, cp		<0.5mm ^φ , rarely euhedral crystal of octahedron	29
Kuratani	Fukushima	Permian	Bedded	<u>tep</u> , <u>rhd</u> , <u>cu</u> , rhc, hs, ms, bem			35
Dainichizawa	Tochigi	"	"	hs, rhc			28
Hokkōji	"	"	"	rhc, all, sol, jb, <u>tep</u> , sx, ws			12
Jūniyashima	"	"	"	rhd, <u>tep</u> , rhc, hs, bem, all, ms			10
Kaso	"	"	"	<u>tep</u> , <u>rhc</u> , <u>spt</u> , rhd, all, gx, ms		<1mm ^φ , rarely euhedral crystal of octahedron, spinel type twinning	10, 23
Kuranosawa	"	"	"	hs, bar, rhc, bem, all, <u>tep</u> , rhd, ms			10
Kyūrasawa	"	"	"	rhc, ms			6
Nomine	"	"	"	rhd, <u>spt</u> , qz, gx, rhc, hs, ms			10
Takahira	"	"	"	<u>tep</u> , rhc, rhd, spt, sp, cp, py			10, 17
Takanosu	"	"	"	<u>tep</u> , rhd, rhc, spt, py, cp, gn, sp		black granular aggregate	13
Atago	Gumma	"	"	rhc, hs, ms			6
Hagidaira	"	"	"	<u>rhd</u> , <u>spt</u> , <u>rhc</u> , <u>dan</u> , <u>qz</u> , <u>po</u> , <u>tep</u> , <u>all</u> , ms, <u>pyp</u>		emulsion texture of pyrrhotite exsolution	9, 31
Hanawa	"	"	"	rhc, bem, gx, <u>all</u> , <u>tep</u> , rhd, spt, gx			9
Konakayama	"	"	"	rhd, py, sp			6
Kurosakaishi	"	"	"	rhd			6
Kurumazawa	"	Tertiary	Vein	rhc, rhd			36
Mogurazawa	"	Permian	Bedded	rhc, bar, qz, bn, tet			15
Ritō	"	"	"	<u>spt</u> , <u>rhd</u> , <u>tep</u> , <u>gx</u> , <u>rhc</u> , <u>pyp</u> , hs			9
Sanyō	"	"	"	rhd			6
Hamayokogawa	Nagano	" (R)	"	all, rhc, hs, ms, rhd, jb, <u>tep</u>			33
Yagisawa	"	"	"	rhd, <u>tep</u> , <u>spt</u> , <u>all</u> , rhc			39
[Hazu District]	Aichi	late Paleozoic-early Mesozoic (R)	"	<u>rhd</u>			11
Taguchi	"	" (R)	"	qz, rhc, <u>tep</u> , ms, jb, gx, dan		1-2mm ^φ , rarely euhedral crystal of octahedron	16, 23
Ioi	Shiga	Permian	"	bem, <u>tep</u> , hs, rhc, all, ms, rhd		1mm ^φ , cubic crystal	26, 35
Takashima	"	"	"	pxm, rhc			36
Yaei	"	"	"	rhc, rhd, <u>tep</u> , bem, qz			36
Yamada	Mie	late Paleozoic-early Mesozoic (R)	"	<u>tep</u> , rhd			36
Yamanaka	Hyōgo	Miocene	Vein	rhd, <u>tep</u> , <u>spt</u> , <u>py</u> , bem, rhc, pxm		color zoning (dark brown-dark green)	35, 38
Mizutani	Tottori	middle-late Paleozoic (Sg)	Bedded	<u>rhd</u> , <u>tep</u> , <u>spt</u> , <u>pyp</u>		<5mm ^φ	35, 36
Ōidani	"	" (Sg)	"	<u>tep</u> , rhc, rhd			32
Toyoka	Shimane	Tertiary	Vein	rhd, rhc, <u>tep</u> , bem, dan, <u>py</u> , <u>sp</u> , <u>cp</u>			36
Fukumaki	Yamaguchi	late Paleozoic-early Mesozoic (R)	Bedded	<u>tep</u> , rhc, <u>gx</u> , <u>pyp</u> , ms, rhd, all, bem			7
Furujuku	"	Permian	"	<u>tep</u> , rhc, rhd, <u>spt</u> , dan, <u>pyp</u>			35
Hata	"	"	"	<u>rhd</u> , <u>py</u> , mac		<3mm ^φ , poikilitic texture with rhodonite	35, 36
Kinkō	"	"	"	rhd, <u>tep</u> , <u>spt</u> , all, pxm			8, 14
Kusugi	"	"	"	<u>tep</u> , rhd, <u>spt</u> , <u>pyp</u> , pxm, rhc, bem	6.9		14, 36, 37
Tennō	"	"	"	rhd, <u>tep</u> , <u>spt</u> , <u>gx</u> , <u>pyp</u> , sol, hs, ms			36
Tsutsumi	"	"	"	rhd, <u>tep</u> , <u>spt</u> , dan, rhc			8
Wagi	"	"	"	rhd, <u>tep</u> , rhc, all, pxm			36
Furumiya	Ehime	late Paleozoic (Sw)	"	hs, rhc, rhd, ms, <u>spt</u>	0.0		5
Iwato	Miyazaki	Permian	"	<u>tep</u> , rhc, rhd, bem, dan			35, 36
Shimozuru	"	"	"	<u>tep</u> , hs, <u>pyp</u> , <u>gx</u> , rhd, <u>spt</u> , dan			36
Nishikata	Kagoshima	"	"	rhd, <u>tep</u> , hs, rhc			4

* : According to Hirokawa (Chief ed.) (1978)

(R) : Ryōke metamorphic rocks

(Sg) : Sangun

(Sw) : Sambagawa

** : Underlines showing intimate paragenesis with alabandite

Abbreviations

alb: alabandite	jb: jacobsonite	qz: quartz
all: alleghanyite	ms: manganosite	rhc: rhodochrosite
bar: barite	mac: marcasite	rhd: rhodonite
bem: bementite	cu: native copper	sol: sonolite
bn: bornite	pw: penwithite	spt: spessartine
brn: braunite	py: pyrite	sp: sphalerite
cp: chalcopyrite	pyc: pyrochroite	sx: sussexite
dan: dannemorite	pyp: pyrophanite	tep: tephroite
gx: galaxite	pyr: pyrrhotite	tet: tetrahedrite
gn: galena	pxm: pyroxmangite	ws: wiserite
hs: hausmannite	po: pyrrhotite	

† : Calculated from the given d(022) by using the calibration equation of Ishida (1976);
a₀ = 5.2234 - 0.001638 (mol. % FeS)

References

- Harada (1954a)
- (1954b)
- (1954c)
- Hatae, Shirozu, & Momoi (1965)
- Hattori & Harada (1960)
- Hayashi & Igarashi (1962)
- Hirowatari (1961)
- (1964)
- & Takeda (1962a)
- & — (1962b)
- Ito & Sakurai (1947)
- Kato & Matsubara (1980)
- , Nakama, & Matsumoto (1965)
- Lee (1955)
- Matsubara & Kato (1977)
- Miyamoto, Otsu, & Kawano (1962)
- , Takase, & Maruyama (1954)
- Nambu (1965)
- & Tanida (1964)
- , —, Kitamura, & Kumagai (1976)
- , —, Oikawa, Kumagai, & Nasukawa (1973)
- Saito, Bamba, Sawa, Narita, Igarashi, Yamada, & Satoh (1967)
- Sakurai (1956)
- Sato, Fukuda, & Wada (1957)
- Shinoda, Sakai, Koono, & Kikuchi (1974)
- Shirozu (1949)
- Suzaki, Urashima, & Hayakawa (1969)
- Tozuka & Kobayashi (1964)
- Watanabe (1939)
- Watanabe (1959)
- , Yui, & Kato (1970)
- Yasuda (1965)
- Yoshie & Hirowatari (1978)
- Yoshimura (1937)
- (1967)
- (1969)
- & Momoi (1961)
- & — (1964)
- & Yoshinaga (1959)

pyrometasomatic deposit type, *i.e.*, the bedded-type manganese deposits in the "Chichibu Paleozoic Formation" metamorphosed highly by intrusion of later granitic rocks, in which alabandite is associated with rhodochrosite, manganese silicates (*e.g.*, rhodonite, tephroite, alleghanyite), and manganese oxides (*e.g.*, hausmannite, manganosite) and commonly includes minute euhedral or granular grains of chalcopyrite, pyrite, and pyrrhotite with the emulsion structure. They have assumed that the former had formed at lower temperature than the latter.

There are a few morphological studies on euhedral alabandite, but it is known to occur very rarely in nature (SHIROZU, 1949; HARADA, 1954a,c; SAKURAI, 1956).

Several chemical composition data of alabandite have been reported, but the analyzed values seem to be unreliable because the analyzed samples were impure. Therefore, the values of FeS mol.% in alabandite calculated from the given $d(022)$ values by using the calibration equation of ISHIDA (1976) are also shown for reference in Table 1.

B. Synthetic alabandite

Alabandite does not depart measurably from stoichiometric composition of MnS and remains stable to about 1610°C (HANSEN and ANDERKO, 1960). There

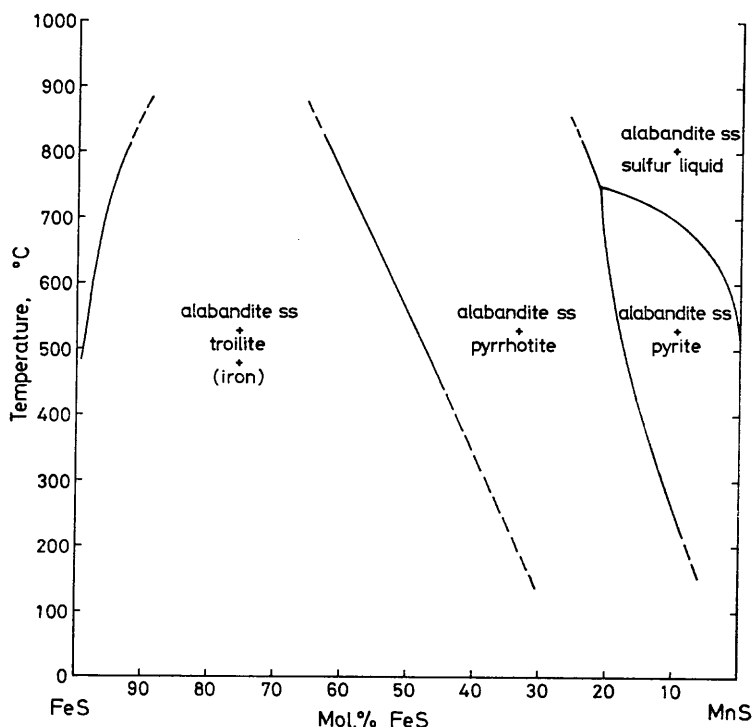


Fig. 1. Composition of alabandite solid solutions in equilibrium with troilite (+iron), pyrrhotite, pyrite, or sulfur liquid after SUGAKI and KITAKAZE (1972).

are several experimental studies of the systems including alabandite, *e.g.*, the system FeS-MnS by SHIBATA (1928) from a standpoint of the steel metallurgy and the system CaS-MgS-MnS-FeS by SKINNER and LUCE (1971) from the mineralogy of enstatite chondrites. The first study for the purpose of direct use in estimating the conditions of ore formation was made by SUGAKI and KITAKAZE (1972) in the system Mn-Fe-S. They have investigated in detail the phase equilibrium relations along the MnS-FeS join of the system by using the rigid and collapsible tube techniques and obtained relation which is very similar to that of the sphalerite solid solution in the system Fe-Zn-S. The gentle slope of the curve of the alabandite+pyrite+pyrrhotite assemblage on a composition-temperature plane shown in Figure 1, which differs from the curve of sphalerite (SCOTT and BARNES, 1971), indicates that the alabandite solvus is useful as a geothermometer. Moreover, ISHIDA *et al.* (1977) have presented the fugacity of S₂-composition diagram for the divariant assemblage of pyrrhotite+alabandite in the range 500–800°C.

III. Locality and manganese deposits

In this study, alabandite has been identified in the samples from nineteen localities as shown in Figure 2. Only three of these, *i.e.*, Nakanoyama, Shōwa, and Fukadani mines are new occurrences. The locations of mines, lithofacies of wall rocks, and the major ore minerals are listed in Table 2.

In the Inakuraishi, Mori, and Yamanaka mines, epithermal fissure filling manganese veins occur in the Neogene volcanic field and their major constituents are rhodochrosite.

The Hamayokogawa, Yamada, and Fukumaki mines are located in the Ryōke metamorphic belt. They are Paleozoic to Mesozoic bedded-type manganese deposits and the last two deposits consist mainly of manganese silicates which can be regarded as thermally metamorphosed products by the intrusion of Cretaceous granitic rocks. The deposit of Hamayokogawa mine is situated in the outer zone of the Ryōke metamorphic belt and it is hardly affected by later thermal metamorphism. Major constituents are fine-grained alleghanyite, hausmannite, and rhodochrosite.

The Furumiya mine, as a bedded-type deposit, is found in the Sambagawa metamorphic rocks. The deposit is considered to have been affected by the Neogene volcanism. Although the major constituent of the deposit consists generally of braunite, alabandite occurs in the ores of rhodochrosite, hausmannite, and manganese silicates which partially replace the braunite ore.

The ore deposits of the other twelve mines, belonging to Permian to Jurassic bedded-type deposits, are intercalated in the "Chichibu Paleozoic Formation". The deposits of Hijikuzu, Nodatamagawa, Kaso, Hagidaira, Fukadani, Kusugi, and Tsutsumi mines have been thermally metamorphosed by the intrusion of the Cretaceous granitic rocks and consist mainly of manganese silicate ores. The deposit of Shimozuru mine has suffered presumably the thermal effects by the Neogene granitic intrusion. The major ore is similarly made up of

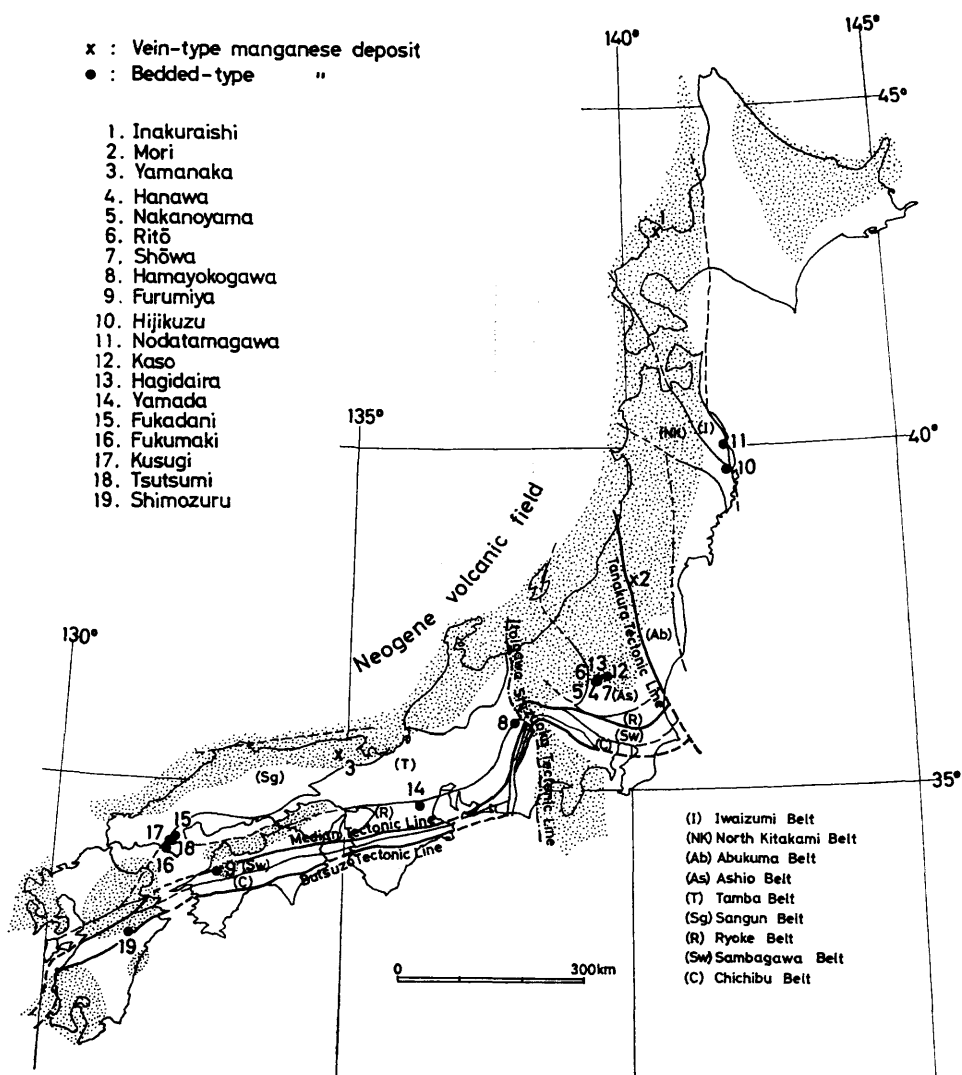


Fig. 2. Location of manganese mines from which samples were taken for this study. Neogene volcanic field and some pre-Neogene geotectonic division are quoted from HIROKAWA (Chief ed.) (1978).

manganese silicates. The deposits of Hanawa, Nakanoyama, Ritō, and Shōwa mines occur in none to weakly metamorphosed sediments and consist mainly of rhodochrosite.

IV. Experimental methods

All the samples obtained from the above deposits were examined microscopically under transmitted and reflected lights in order to identify alabandite. Then the constituents of the selected samples were identified by means of X-ray

Table 2. General features of the manganese deposits occurring alabandite used in this study.

Mine	Location	Age	Type	Wall rocks	Chief constituents
1. Inakuraishi	30km W of Otaru City, Hokkaido Prefecture	Miocene	Vein	propylite and tuff breccia	rhc,alb
2. Mori	28km SW of Yamagata City, Yamagata Prefecture	"	"	granodiorite	rhc
3. Yamanaka	17km S of Toyooka City, Hyōgo Prefecture	"	"	rhyolitic tuff	rhd,rhc,alb
4. Hanawa	16km N of Kiryū City, Gumma Prefecture	Permian	Bedded	massive chert and bedded chert	rhc,bem,pxm
5. Nakanoyama	15km N of Kiryū City, Gumma Prefecture	"	"	"	rhc,bem,all
6. Ritō	17km N of Kiryū City, Gumma Prefecture	"	"	"	rhc,bem
7. Shōwa	"	"	"	"	rhc,bem,hs
8. Hamayokogawa	25km S of Matsumoto City, Nagano Prefecture	" (R)	"	"	all,hs,rhc
9. Furumiya	15km S of Matsuyama City, Ehime Prefecture	late Paleozoic (Sw)	"	piemontite quartz schist and quartzite	brn,rhd,rhc,hs,alb
10. Hijikuzu	16km NW of Miyako City, Iwate Prefecture	Jurassic	"	hornfels of massive chert and bedded chert	pxm,rhd,tep,brn
11. Nodatamagawa	16km SE of Kuji City, Iwate Prefecture	Permian-early Mesozoic	"	"	rhd,tep,hs,pyc
12. Kaso	12km NW of Kanuma City, Tochigi Prefecture	Permian	"	"	rhc,tep,rhd
13. Hagidaira	19km N of Kiryū City, Gumma Prefecture	"	"	"	rhd,alb,tep
14. Yamada	25km W of Tsu City, Mie Prefecture	late Paleozoic- early Mesozoic (R)	"	schistose hornfels of bedded chert	rhd,tep,alb
15. Fukadani	16km W of Iwakuni City, Yamaguchi Prefecture	Permian	"	hornfels of massive chert	rhd,pxm,rhc
16. Fukumaki	6km E of Kudamatsu City, Yamaguchi Prefecture	late Paleozoic- early Mesozoic (R)	"	hornfels of biotite schist and massive chert	rhd,tep,alb
17. Kusugi	23km WSW of Iwakuni City, Yamaguchi Prefecture	Permian	"	hornfels of massive chert and bedded chert	rhd,tep,spt,alb
18. Tsutsumi	18km SW of Iwakuni City, Yamaguchi Prefecture	"	"	"	rhd,pxm,tep,spt
19. Shimosuru	30km NW of Nobeoka City, Miyazaki Prefecture	"	"	hornfels of massive chert	tep,rhd,alb,dan

Abbreviations are the same as shown in Table 1.

diffraction. Chemical composition of alabandite and the associated minerals were quantitatively determined by electron probe microanalysis.

The quantitative analyses were carried out in most cases for Mn, Fe, and S in alabandite, for Zn, Fe, Mn, and S in sphalerite, for Mn, Fe, Ca, Mg, Al, Ti, and Si and, when necessary, Na and K in oxides and silicates, and for Mn, Fe, Ca, and Mg in carbonates.

The analytical conditions of the electron probe microanalyser (Japan Electron Optics Laboratory Co., Ltd., Model JXA-5A with 40° take-off angle) were as follows: for sulfides, the accelerating voltage, specimen current, and electron beam diameter were 20 kV, 0.015 μ A (on pure iron), and 2 to 3 μ , respectively. The characteristic X-rays used were S-K α (analysing crystal: PET, standard specimen: synthetic MnS or CuFeS₂), Mn-K α (LiF, synthetic MnS), Fe-K α (LiF, synthetic FeS or CuFeS₂), and Zn-K α (LiF, metal Zn). For oxides, silicates, and carbonates, the accelerating voltage, specimen current, and electron beam diameter were 15 kV, 0.015 μ A (on pure iron), and 1 to 2 μ , respectively. The characteristic X-rays employed were Mn-K α (LiF, natural MnO), Fe-K α (LiF, synthetic Fe₂O₃), Ca-K α (PET, synthetic CaSiO₃), Mg-K α (KAP, synthetic MgO), Al-K α (RAP, synthetic Al₂O₃), Ti-K α (LiF, synthetic TiO₂), Si-K α (RAP, synthetic CaSiO₃), Na-K α (RAP, natural NaAlSi₃O₈), and K-K α (PET, natural KAlSi₃O₈). Corrections based on the Sweatman and Long method (ZAF method) were used for sulfides and the Bence and Albee method for oxides, silicates, and carbonates.

V. Occurrence and paragenesis

The mole percent FeS and the grade of pyrrhotite exsolution in alabandite, and the relative amount of principal constituents in the alabandite specimens are summarized in Figure 3. The amount of other contents except for MnS and FeS in alabandite is generally so small that the chemical composition of alabandite can be expressed as the mol.% FeS. The result shows that the FeS content in alabandite varies continuously from 0.2 to a maximum of 13.5 mol.% and has intimate relations with the coexisting minerals. The chemical analyses of alabandite are shown in Appendix I-A.

The mode of occurrence, chemical composition, and paragenetic relation of alabandite in each sample are described as follows.

A. Alabandite from vein-type manganese deposits

In the samples from the vein-type deposits, alabandite is commonly associated with rhodochrosite and quartz, and usually occurs as granular coarse grains with heterogeneous composition. It usually shows no exsolution texture. The FeS content in alabandite is 0.6 to 5.8 mol.% and the differences among those from three deposits are considerably small.

1. Inakuraishi mine

The sample (R.C.) was collected from the point of W50m at 7L of Tsūdō

vein. It is an aggregate ore of coarse-grained (more than 2 mm in size) rose pinkish rhodochrosite and dark brownish alabandite, which is associated with small amount of quartz. The sulfides and sulfosalts such as euhedral or subhedral marcasite (partly pyrite), petal-like wurtzite (partly sphalerite), galena, chalcopyrite, miargyrite, pyrargyrite, Mn-bearing fizelyite, Mn·Ag-bearing tetrahedrite, diaphorite, and Mn-bearing andorite occur around the boundaries between alabandite and rhodochrosite or quartz grains. Stibnite occurs as veinlets cutting these minerals, but is invaded by marcasite veinlets. Although the marcasite and wurtzite are considerably of coarse grains up to 1 mm in size, the other sulfides and the sulfosalts are very fine grains less than 0.1 mm.

Under a polarizing microscope, the alabandite frequently shows the color zoning of greenish yellow to reddish brown and no exsolution texture. The FeS content varies extensively from 0.6 to 5.2 mol.% in accordance with the variations of color.

2. Mori mine

The sample (621080) is composed mainly of light pinkish and dark brownish rhodochrosite (up to 2 mm in size) associated with small amount of quartz. The dark brownish one includes abundantly fine grains of alabandite and euhedral marcasite (partly pyrite) less than 0.1 mm in size. Alabandite is out of contact with quartz and has no exsolution texture.

The composition of alabandite varies considerably among the individual grains but is fairly constant within one grain with the range of 1.0 to 5.8 mol.% FeS.

3. Yamanaka mine

Sample (A) is composed mainly of coarse-grained alabandite up to 1 cm. The veinlets of fluorite which is associated with accessory rhodochrosite, rhodonite, and quartz cut through alabandite, and euhedral pyrite occurs in small amount along the boundaries.

Sulfides such as sphalerite, galena, and chalcopyrite are present as minor constituents in or around the grains of alabandite. Although sphalerite shows no exsolution, alabandite contains a little pyrrhotite grains as minute emulsions.

The FeS content of alabandite is 2.4 to 4.4 mol.%.

B. Alabandite from bedded-type manganese deposits

In the samples from the bedded-type deposits, alabandite is associated with a large variety of manganese minerals compared to the vein-type deposits. The composition generally has a tendency to vary in accordance with the kinds of associated minerals. The tendency is evident especially in the case of ores strongly affected by thermal metamorphism. This type of deposits can be subdivided into two cases according to their metamorphic grades.

B-1. None to weakly metamorphosed deposits

In the deposits which are not metamorphosed or very weakly affected, the

Mine	Sample No.	FeS mol.% in alabandite														Exsolution in alb Alabandite	Manganosite Hausmannite	Jacobite	Rhodochrosite	Alleganyite Sonolite	Tephroite	Rhodonite	Pyromangite	Quartz Pyrite Pyrrhotite Sphalerite
		1	2	3	4	5	6	7	8	9	10	11	12	13	14									
Inakuraishi	R.C.	••	••••	••••••	••											x	••		••					••
Mori	621080	••••••••	••			••										x	+		••					••
Yamanaka	A		••	••••												△	••		+			+		••
Hanawa	570733 570739	••					•									x	+	+	••			+		•
Nakanoyama	570746	•••														x	+		••	+				
Ritō	570741 570742 570743	••	••	••												x	+	+	••	••		+	+	
Shōwa	570708 570706 570704 570710 570707 570709	•	•													x	+	+	••	••				•
Hamayokogawa	5208 5205	••	••													x	+	••	••	••				
Furumiya	5812108	••														x	••	••	••		••	+		•
Hijikuzu	621095-1	•														△	+		••	••	••			••
Nodatamagawa	L12-G S.Z. V.C. L12-1,2 V.O.		••	••	••	••	•			•	••	•	••	••	•	x	+	••	••	••	••			••
Kaso	28 29 22-B	••	••	••												x	+	••	••	••	••			
Hagidaira	570728 570730 570717 570719 570720 570724 570718 570716 570721 570725	•	•	•	•											x	+	••	••	••	••			••
Yamada	1			•	•	••										○	+		••	••				••
Fukadani	50122801									•	•	••	•	•	•	⊙	+		••		••			••
Fukumaki	5711516 5711521 571121 571193 571145 5711524 5711109(c) 5711505 571109(b) 571118 571154 571148 571109(a) 571128(a) 5711515 5711503 571159	•	•	•	•	•	•	•	•	•	•	•	•	•	•	•	x	+	••	••	••	••		•
Kusugi	58052607 58052602 58052601									••	•	•	•	•	•	⊙	+		••	••			••	••
Tsutsumi	58052004 58052006 58052015			•	•			••	••	•	•	•	•	•	•	x	+		••	••	••	••		••
Shimozuru	1			••												x	+			••	••			

Fig. 3. Relation between mineral assemblage and chemical composition of alabandite in the manganese mines in this study.

+: relative amount of alabandite and associated minerals, and the more number in increase of abundance.

⊙, ○, △, ×: grade of exsolution in alabandite, large, medium, rare, and none, respectively.

•: showing the presence of pyrite, pyrrhotite, or sphalerite.

ore generally consists mainly of rhodochrosite associated with insignificant amount of alabandite. Moreover the iron content of alabandite is lower than that in highly metamorphosed ores.

1. Hanawa mine

Sample (570733) is composed mainly of fine-grained rhodochrosite and alleghanyite associated with small amounts of manganosite, galaxite, and bementite. The sample (570739) consists mainly of rhodochrosite and pyroxmangite and is associated with small amounts of spessartine and pyrophanite. Very minor amount of alabandite is disseminated in the rhodochrosite ores. Alabandite takes granular or irregular shape and is up to 0.2 mm in size. It contains no exsolved mineral.

The FeS content of alabandite is 0.3 to 0.6 mol.% for the sample (570733), and 5.3 to 5.4 mol.% for (570739).

2. Nakanoyama mine

Sample (570746) is composed mainly of fine-grained rhodochrosite and alleghanyite and is associated with small amount of galaxite. Minor amount of alabandite occurs in rhodochrosite as dispersed grains which are granular and less than 0.1 mm in size. It shows no exsolution texture.

The FeS content in alabandite ranges from 0.6 to 1.4 mol.%.

3. Ritō mine

Samples (570741, 570742, 570743) are composed mainly of rhodochrosite associated with various amounts of tephroite, alleghanyite, rhodonite, pyroxmangite, spessartine, bementite, hausmannite, and small amounts of galaxite, pyrophanite, and penwithite. Minor amount of alabandite whose grains are granular and up to 0.4 mm in size and have no exsolution is disseminated in the fine-grained rhodochrosite. It frequently accompanies minute amount of barite.

The FeS content in alabandite is 0.3 to 2.0 mol.%.

4. Shōwa mine

Samples (570708, 570706, 570704, 570710, 570707, 570709) are composed mainly of fine-grained rhodochrosite associated with various amounts of alleghanyite, tephroite, manganosite, bementite, jacobsonite, and small amounts of galaxite, spessartine, hausmannite, sonolite, and pyrophanite. Minor amount of alabandite occurs as dispersed or layered grains in rhodochrosite and in the case of the latter the direction of layers is almost parallel to that of the banded texture in the ore itself. Alabandite is irregular or granular and commonly less than 0.3 mm in grain size and accompanies minor amounts of barite, pyrite, and invariably Ni-bearing minerals such as millerite, gersdorffite, pentlandite, and breithauptite.

The FeS content in alabandite is 0.2 to 6.6 mol.%. Exsolved pyrrhotite is found in the alabandite from sample (570709) which has the highest FeS content.

5. Hamayokogawa mine

Although the deposit is located in the outer zone of the Ryōke metamorphic belt, it has hardly been affected by the later thermal metamorphism.

The samples (5208, 5205) are composed mainly of fine- to medium-grained rhodochrosite and alleghanyite, associated with notable amount of jacobsite and small amounts of bementite and barite. Jacobsite occurs as very minute grains with layered structure. A small amount of alabandite is scattered in rhodochrosite and alleghanyite. It is less than 0.1 mm in grain size and takes no exsolution.

The FeS content in alabandite is 0.2 to 0.7 mol.%.

6. Furumiya mine

The deposit is found in the Sambagawa metamorphic belt. The ore containing alabandite shows rather unusual occurrence, which is described below.

Sample (5812108) which is considered to have formed by reduction of braunite-quartz ore, shows zonal structure forming rings which are several centimeters across. They are composed of hausmannite-rhodochrosite-alabandite-tephroite-rhodonite-quartz from the center outward. The zone of alabandite is associated with barite, euhedral spessartine, and small amounts of galena, pyrite, and chalcopyrite. Alabandite is up to 0.3 mm in size, and has irregular myrmekitic texture but no exsolution.

The FeS content in alabandite is 0.2 to 0.6 mol.%.

B-2. Moderately to highly metamorphosed deposits

In the deposits moderately to highly affected by thermal metamorphism, the ore generally consists of manganese silicates associated with considerable amount of alabandite. Moreover the iron sulfides are frequently and abundantly accompanied with it. The iron content in the alabandite is relatively higher than that from unmetamorphosed deposits.

1. Hijikuzu mine

Sample (621095-1) comprises coarse-grained granoblastic rhodochrosite and tephroite, and is associated with small amounts of alleghanyite and sonolite. Rhodochrosite is turbid. Manganese silicates are almost all replaced by bementite. Alabandite commonly occurs as granoblastic aggregates with rhodochrosite and tephroite, but partly as veinlets. The former contains little emulsions of pyrrhotite and chalcopyrite, but the latter no exsolved minerals. It rarely shows optical anisotropy under the transmitted light. Minor amount of pyrite also occurs as veinlets cutting these minerals.

The FeS content in alabandite is 1.4 mol.%.

2. Nodatamagawa mine (Kiri-hata deposit)

Samples (V.C., V.O.) were collected from the point of S500 at 0mL of Kiri-hata deposit. The sample (V.C.) is composed mainly of irregular grained (up to 0.3 mm in size) alabandite and spessartine, associated with tephroite, rhodonite, and small amounts of Ba-bearing phlogopite, pyrophanite, chalcopyrite,

pyrite, and cobaltite. The sample (V.O.) is composed mainly of irregular grained rhodonite around 0.1 mm in size with small amounts of spessartine, pyrophanite, and huebnerite. Sulfides occur along the grain boundaries of rhodonite. They commonly accompany turbid rhodochrosite, and consist of pyrite, marcasite, chalcopyrite, sphalerite, and alabandite. Sphalerite contains lamellar or dotted grains of chalcopyrite, pyrrhotite, and pyrite. In both samples, alabandite has no exsolution texture. FeS content is 4.2 to 5.4 mol.% for the former, and 11.0 to 12.1 mol.% for the latter.

Sample (L12-G) is composed mainly of granoblastic (around 0.3 mm in size) rhodochrosite, tephroite, and alabandite, associated with minor amounts of galaxite, pyrophanite, and pyrite. Alabandite contains the content of 2.6 to 2.9 mol.% FeS and has no exsolution.

Sample (S.Z.) is composed mainly of granoblastic (around 1 to 2 mm in size) tephroite and alabandite associated with small amounts of galaxite, rhodochrosite, and bementite. Minor amounts of sulfides such as sphalerite, chalcopyrite, and niccolite occur along the grain boundaries of alabandite. Although sphalerite has no exsolution, alabandite contains small amount of emulsions of pyrrhotite. FeS content in alabandite is in the range of 2.4 to 3.4 mol.%.

Sample (L12-1,2) is massive aggregate ore composed of alabandite, pyrrhotite, and Mn-bearing magnetite around 0.3 mm in size. They accompany tephroite, chalcopyrite, pyrite, and small amounts of rhodochrosite, spessartine, jacobsonite, bementite, pyrophanite, and minor amounts of sphalerite and scheelite. The boundaries and rims between pyrrhotite and Mn-bearing magnetite grains are commonly replaced by pyrite in part and very rarely by hematite. Alabandite usually shows the exsolution texture of pyrrhotite emulsions. FeS content in alabandite varies from 2.8 to 12.3 mol.%.

3. Kaso mine

Samples (28, 29, 22-B) are composed mainly of fine-grained rhodochrosite and alleghanyite associated with tephroite, jacobsonite, hausmannite, manganosite, bementite, and galaxite. Small amount of alabandite occurs as fine and granular grains scattered in these minerals. It has no exsolution texture.

The FeS content in alabandite is 0.4 to 2.4 mol.%.

4. Hagidaira mine

The samples can be subdivided into three types according to the major constituents.

(1) *Rhodochrosite-manganosite ore (570728, 570730, 570717)*

The ore consists of alternating two bands in each thickness of several millimeters and one of which is composed mainly of manganosite, rhodochrosite, alabandite, and tephroite and the other is of tephroite, rhodochrosite, and galaxite. Manganosite is usually rimmed with very fine-grained hausmannite. Tephroite is frequently accompanied with small amount of sonolite. Alabandite is 0.1 to 0.3 mm in grain size. It occurs commonly as granular grains and partly

as veinlets. It is rarely accompanied with chalcopyrite.

The FeS content in alabandite is 0.3 to 0.6 mol.%.

(2) *Tephroite ore* (570719, 570720, 570724)

The ore shows the banded structure as a whole and is composed mainly of granoblastic alabandite and tephroite associated with rhodonite, sonolite, galaxite, and pyrophanite. Tephroite is partly replaced with bementite. Alabandite is occasionally accompanied with turbid rhodochrosite, and small amounts of pyrite, pyrrhotite, sphalerite, and chalcopyrite. It is 0.1 to 1 mm in grain size and has minute emulsions of pyrrhotite as a product of exsolution.

The FeS content in alabandite is 1.0 to 3.0 mol.%.

(3) *Rhodonite ore* (570718, 570716, 570721, 570725)

The ore contains the largest quantity of alabandite in this mine, and is composed mainly of alabandite and subhedral coarse-grained (up to 1 cm in size) rhodonite associated with turbid rhodochrosite, spessartine, bementite, and small amounts of pyroxmangite, quartz, and pyrophanite. Alabandite commonly occurs as disklike or spheroidal aggregates usually associated with small amounts of pyrite, pyrrhotite, chalcopyrite, and sphalerite. It shows irregular grains with 0.3 to 4 mm across, and commonly contains exsolved product of pyrrhotite.

The FeS content in alabandite is 1.8 to 10.1 mol.%.

5. Yamada mine

Sample (1) is composed mainly of granoblastic tephroite, rhodochrosite, and alabandite, and is associated with small amounts of spessartine and pyrophanite. Alabandite is accompanied with minor amounts of pyrrhotite, sphalerite, gersdorffite, and niccolite. It is less than 1 mm in grain size and has pyrrhotite exsolution.

The FeS content in alabandite is 4.3 to 5.9 mol.%.

6. Fukadani mine

Sample (50122801) is composed of coarse-grained pyroxmangite, rhodochrosite, and quartz associated with small amounts of spessartine, pyrophanite, and huebnerite. Alabandite is commonly accompanied with pyrrhotite, chalcopyrite, pyrite, sphalerite, gersdorffite, and niccolite. It occurs as scattered grains less than 1 mm in size and also contains many pyrrhotite exsolution.

The FeS content in alabandite is 9.5 to 13.5 mol.% which is a maximum value in this study.

7. Fukumaki mine

The samples can be divided into two types according to the major constituents.

(1) *Tephroite-rhodochrosite ore* (5711516, 5711521, 571121, 571193, 571145, 5711524, 5711109(c), 5711505, 5711109(b), 571118, 571154, 571148, 5711109(a))

The ore is composed usually of tephroite and rhodochrosite associated with

various amounts of alabandite, sonolite, alleghanyite, spessartine, galaxite, rhodonite, Mn-bearing amphibole, bementite, pyrophanite, and welinite. Alabandite is frequently accompanied with small amounts of pyrite, sphalerite, and Ni-Co-As-S minerals. It has irregular or granular shape with up to 1 mm in grain size and has no exsolution product.

The FeS content in alabandite is 0.3 to 3.6 mol.%.

(2) *Rhodonite ore (5711128(a), 5711515, 5711503, 571159)*

The ore is composed generally of rhodonite associated with alabandite, tephroite, rhodochrosite, spessartine, pyrophanite, and bementite. Alabandite is accompanied with small amounts of pyrite, sphalerite, and Ni-Co-As-S minerals. It is irregular or granular in shape and is up to 1 mm in grain size. It has no exsolution except in sample (5711503).

The FeS content in alabandite is 3.0 to 8.2 mol.%.

8. Kusugi mine

Samples (58052607, 58052602, 58052601) are composed mainly of very coarse-grained (up to 2 cm in size) rhodonite in which alabandite is scattered, associated with small amounts of spessartine, rhodochrosite, pyrophanite, and quartz. Alabandite is up to 3 mm in grain size and is commonly accompanied with sphalerite, pyrrhotite which is partly replaced by pyrite, chalcopyrite, and arsenopyrite. Sphalerite has no exsolution texture, but alabandite contains exsolved pyrrhotite up to 50 μ in grain size, which is the largest in this study and occasionally shows subhedral forms.

The FeS content in alabandite is 9.1 to 13.0 mol.%.

9. Tsutsumi mine

Samples (58052004, 58052006, 58052015) are composed mainly of tephroite, rhodochrosite, and pyroxmangite associated with spessartine, pyrophanite, and rarely with small amount of huebnerite. Alabandite is irregular or granular in shape and less than 0.3 mm across, and forms a thin band. It is commonly accompanied with minor amounts of pyrite, sphalerite, chalcopyrite, gersdorffite, and niccolite. No exsolution is found in the alabandite.

The FeS content in alabandite ranges from 4.5 to 10.3 mol.%.

10. Shimozuru mine

Sample (1) is composed mainly of spessartine, tephroite, and alabandite whose grain sizes are about 0.1 mm, associated with rhodonite, tirodite, and phlogopite. Alabandite is irregular or granular in grain shape and is accompanied with minor amount of chalcopyrite. It does not have exsolution texture.

The FeS content in alabandite is 4.2 to 4.7 mol.%.

C. Summary

The characteristics of the modes of occurrence, paragenetic relations, and chemical composition of alabandite from each deposit in this study are summarized in Table 3.

Table 3. Summary of the modes of occurrence, paragenetic relations, and chemical composition of alabandite.

	Grade of thermal metamorphism	Mine	Associated minerals*	FeS mol.% in alb	Amount of alb	Exsolution in alb	py	po	Ni-Co- As-S- minerals
Vein-type (Tertiary)		Inakuraishi	rhc						
		Mori	qz	0.6-5.8	‡	x	o	x	x
		Yamanaka	(rhd)						
Bedded-type (Mesozoic -Paleozoic)	None -weak	Hanawa	rhc	0.2-0.9	+	x	x	x	Δ
		Nakanoyama	ms and/or hs (all) (tep) (jb)						
		Ritō	rhc	0.2-6.6	+	x	x	x	Δ
		Shōwa	(all) (tep) (pxm) (rhd) (jb)						
	Moderate -strong	Hamayokogawa							
		Furumiya							
		Hijikuzu	ms and/or hs	0.3-0.6	‡	x	x	x	Δ
		Nodatamagawa	rhc (all) (tep) (jb)						
		Kaso	tep	0.3-3.6 [†]	‡	Δ	Δ	x	Δ
		Hagidaira	rhc (sol) (all) (jb)						
		Yamada		0.6-13.5	‡	o	o	o	Δ
		Fukadani	rhd and/or pxm (tep) (rhc) (qz) (sol)						

* : The minerals parenthesized do not always
coexist in an ore body.

† : except for the sample of Nodatamagawa(L12-1,2)
Abbreviations are the same as shown in Table 1.

+ : the more number in increase of
abundance

o, Δ, x : grade of exsolution in
alabandite, abundant, common, and
rare, abundance of minerals, large,
medium, and rare to none, respectively

Because alabandite from the vein-type deposits generally has heterogeneous composition not only within one grain but among different grains and contains no exsolution products, it is interpreted to have preserved the conditions of the ore-forming process to a considerable degree. Moreover, it is considered that the stability field of alabandite will probably be determined by the f_{CO_2} , f_{O_2} , and f_{S_2} which controll the reactions among rhodochrosite, alabandite, and rhodonite during ore deposition.

In the bedded-type deposits which have not been affected substantially by thermal metamorphism, the sulfur-bearing minerals occurring in the ore bodies are usually very small amounts of alabandite, barite, and Ni-Co-As-S minerals. Thus, it implies that the amount of sulfur itself was insufficient when the deposits had been formed. During the course of thermal metamorphism, the amounts of sulfur-bearing minerals, especially alabandite, tend to increase. These facts obviously suggest that the additional sulfur was introduced from the wall rocks. Moreover, with the increase of temperature, the mineral assemblages changed and zonal distribution of ore minerals became more distinct, *i.e.*, Mn-oxide ore (consisting mainly of manganosite and/or hausmannite), tephroite ore, and rhodonite ore (containing pyroxmangite ore) in Table 3. It seems that the differences in the mineral assemblages in an ore body produced the diverse ranges of f_{O_2} , f_{CO_2} , and f_{S_2} as buffers in each zone. Consequently, notable variations in the chemical composition of alabandite might reflect the depositional conditions. Alabandite in the highly metamorphosed deposits has generally homogeneous composition in each zone. However, some variations are observed in the composition of alabandite because of extensive exsolution of pyrrhotite during the retrogressive process by annealing.

Judging from the great varieties of the associated minerals and their wide distribution, alabandite is expected to have considerably extensive stability fields. Besides, its chemical composition has characteristic values in relation to its paragenesis and this is taken as an evidence that each mineral assemblage controls the composition of alabandite.

Therefore, the compositional relations between alabandite and the associated sulfides, oxides, silicates, or carbonates are important and the results of the study are reported in the following sections.

VI. Compositional relation between alabandite and associated minerals

A. Sulfides

Alabandite in the vein-type deposits is commonly associated with the sulfosalts containing silver, antimony, and so on, while that in the bedded-type deposits with the sulfides containing nickel, cobalt, arsenic, and so on. Sulfides such as pyrite or pyrrhotite, chalcopyrite, sphalerite, and galena occur in both types and the amount of these minerals is usually very small, but they are important as possible indicators of f_{S_2} . Sphalerite is particularly useful as an indicator of the chemical environment of ore deposition because its FeS content

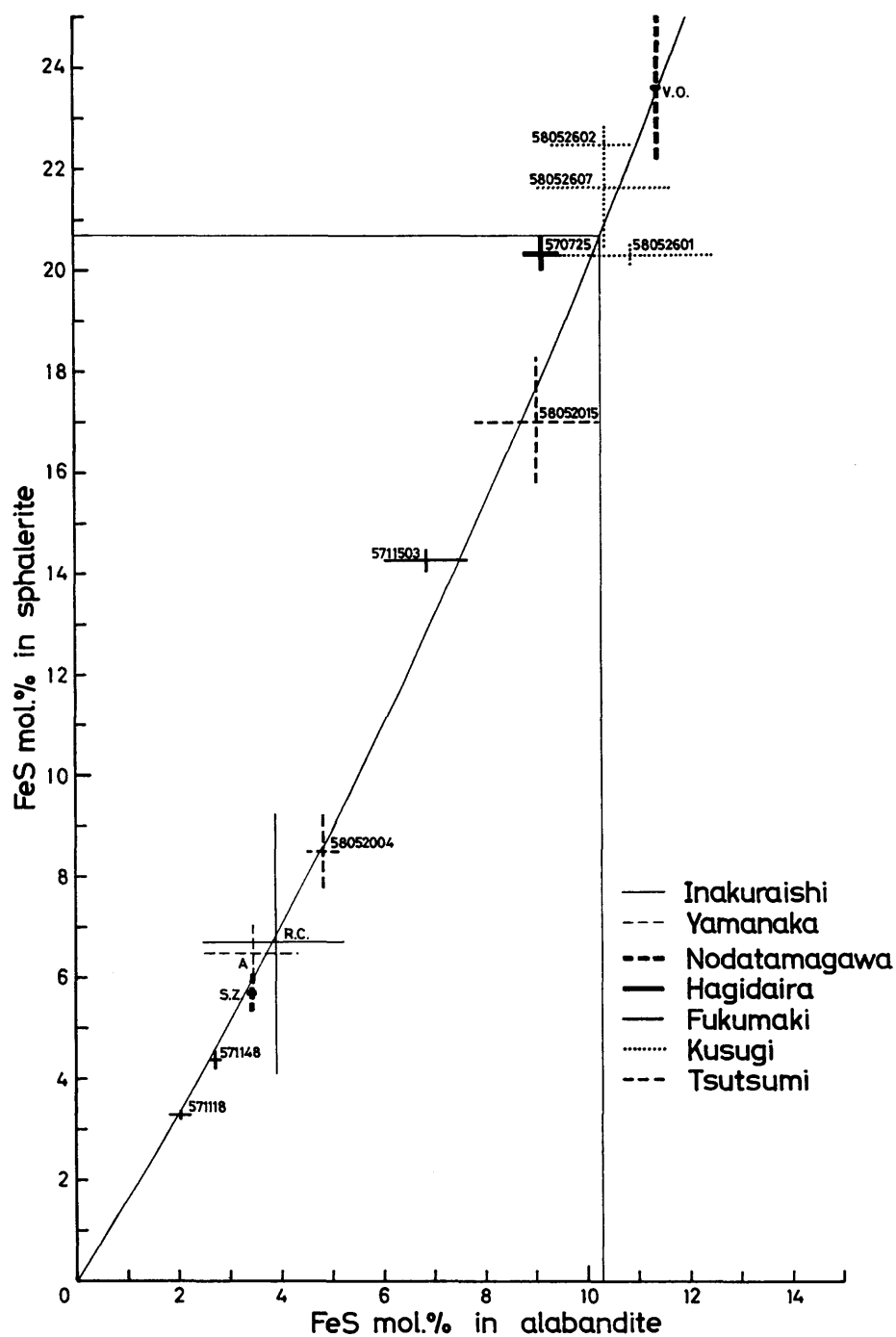


Fig. 4. Relation between iron content in sphalerite and that in alabandite. 20.7 mol.% FeS in sphalerite corresponds to the assemblage, pyrrhotite+sphalerite+pyrite in Zn-Fe-S system below 550°C given by SCOTT and BARNES (1971).

is simultaneously controlled by temperature and fs_2 .

Therefore, the compositional relation between sphalerite and alabandite in the typical samples is examined.

Sphalerite

As the stability field of sphalerite solid solution and its paragenetic relations in the ZnS-MnS-FeS plane of the Zn-Mn-Fe-S system in the manganese deposits of Japan are reported by FUKUOKA and HIROWATARI (1981), the relationship between the FeS content in sphalerite and that in alabandite is considered here.

The samples examined amount to thirteen in all, that is, Inakuraishi (R.C.), Yamanaka (A), Nodatamagawa (S.Z., V.O.), Hagidaira (570725), Fukumaki (571118, 571148, 5711503), Kusugi (58052607, 58052602, 58052601), and Tsutsumi (58052004, 58052015). The chemical analyses of sphalerite are shown in Appendix I-B. Relationship between the FeS content in sphalerite and alabandite whose grains intimately contact each other is represented in Figure 4.

As realized from the figure, there is a close correlation between the FeS content in alabandite and that in sphalerite throughout the above samples. This means probably that the variations of the iron content in both minerals have mutually similar tendencies in relation to sulfur fugacity and temperature within the ranges occurring in nature at least in the stability field of pyrite. Thus, it is presumably difficult to determine the ore formation temperature and fs_2 at once from the values of the iron content in alabandite and sphalerite in the natural samples. Alabandite which occurs within the stability field of pyrrhotite frequently contains exsolutions of pyrrhotite, even when the associated sphalerite has no exsolution products. This indicates that the reaction rate of the former is comparatively faster than that of the latter. If the value of about 10 mol.% is given as the FeS content in alabandite equilibrating with pyrite and pyrrhotite from Figure 4, the forming temperature of about 250°C is obtained by using the data shown in Figure 1. Likewise, if the maximum value of 13.5 mol.% FeS in alabandite obtained in this study is used, the temperature is about 350°C. Therefore, present composition of alabandite might record the state at about 300°C where the exsolution reaction was completed, even though alabandite has primarily formed at higher temperature.

Conversely from the relationship in Figure 4, the iron content in alabandite can be estimated approximately by that in sphalerite in case alabandite does not occur and vice versa.

The other sulfides which bear compositional relations with alabandite are the minerals in the FeAsS-NiAsS-CoAsS system, but the results examined on those minerals have already been reported by FUKUOKA and HIROWATARI (1980a).

B. Manganese oxides

The manganese oxides associated with alabandite consist of manganosite, hausmannite, jacobsite, iwakiite, galaxite, pyrophanite, and Mn-bearing magnetite of which the former three minerals show the most widespread and abundant occurrences in manganese deposits. Although the manganosite rarely forms solid solution in nature, the mineral in the system Mn_3O_4 - Fe_3O_4 , especially jacobsite forms wide range of solid solutions. Because the whole stability field of jacobsite

solid solution and its paragenetic relations in the Mn_3O_4 - MnFe_2O_4 - MnAl_2O_4 and Mn_3O_4 - MnFe_2O_4 -" Mn_2TiO_4 " systems in the natural manganese deposits of Japan have already been reported by FUKUOKA and HIROWATARI (1980b), the relationship between the iron content in alabandite and the minerals in the system Mn_3O_4 - Fe_3O_4 is considered here within the Mn_3O_4 - Fe_3O_4 - MnS - FeS plane of the system Mn-Fe-S-O.

Jacobsite (Mn_3O_4 - Fe_3O_4 system)

The six samples of Hamayokogawa (5208, 5205), Nodatamagawa (L12-1,2), and Kaso (28, 29, 2-B) were examined and the chemical analyses of jacobsonite are shown in Appendix I-C.

The compositional relationship between alabandite and the associated jacobsonite is given in Figure 5, plotted in the Mn_3O_4 - Fe_3O_4 - MnS - FeS plane. Phase relations in the Mn-Fe-S-O system are tentatively shown in Figure 6 in relation to other parageneses observed in nature.

Although the stoichiometric composition of jacobsonite is MnFe_2O_4 , natural jacobsonite generally has the composition shifted a little toward the Mn_3O_4 side. The iron sulfide, which can occur associated with jacobsonite of these compositions, is pyrite and the associated alabandite usually contains less than 2 mol.% FeS. Further, alabandite accompanied with hausmannite contains smaller amount of

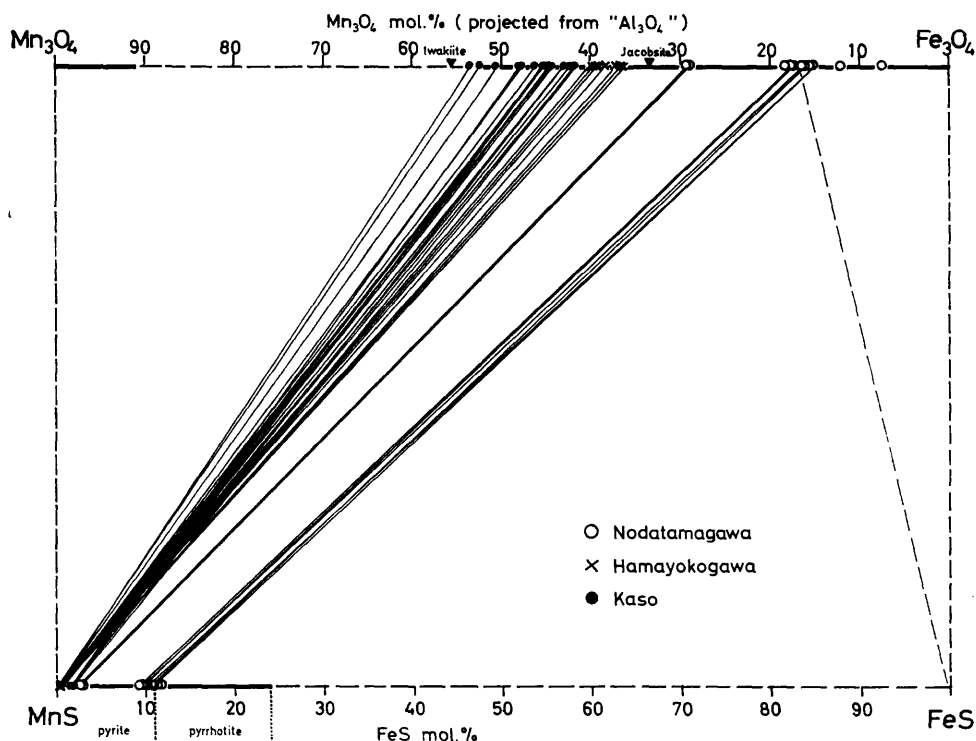


Fig. 5. Relation between iron content in jacobsonite and that in alabandite on the Mn_3O_4 - Fe_3O_4 - MnS - FeS plane of Mn-Fe-S-O system.

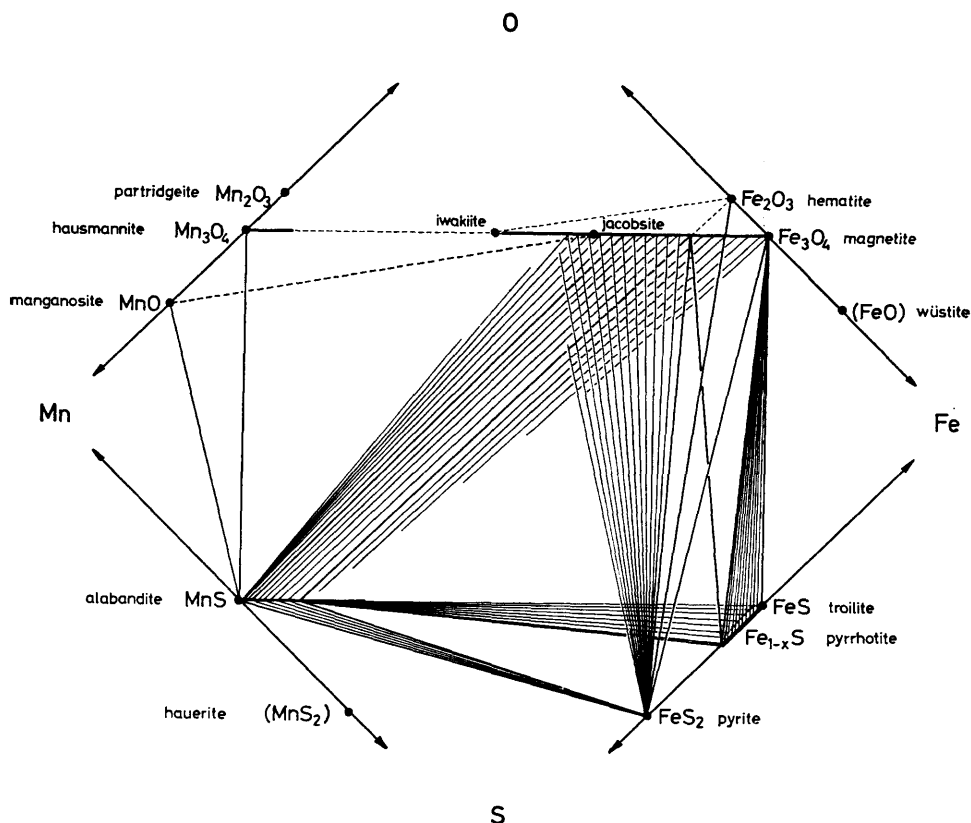


Fig. 6. Possible phase relations in the system Mn-Fe-S-O for the natural manganese deposits.

FeS. This is compatible with the fact that the FeS content of alabandite in the manganosite and/or hausmannite ore is less than 1 mol.% without exception as shown in Table 3.

But when alabandite is associated with jacobsonite or Mn-bearing magnetite having iron-rich compositions, the FeS content increases in proportion to the amount of Fe_3O_4 in the oxide. In the four phase assemblage of pyrrhotite+pyrite+alabandite+jacobsonite observed in the sample of Nodatamagawa (L12-1,2), the iron content in alabandite and jacobsonite is about 11 mol.% FeS and 83 mol.% Fe_3O_4 , respectively. Although no three phase assemblage, alabandite+pyrrhotite+magnetite, was observed in this study, it could be explained that the more abundant iron is dissolved in alabandite.

From the results, it is inferred that the iron in the ore bodies has been preferentially seized into oxides to form jacobsonite, and consequently alabandite was formed with low iron content under the stability conditions of the manganese oxides.

C. Manganese silicates

There are many kinds of manganese silicate minerals associated with

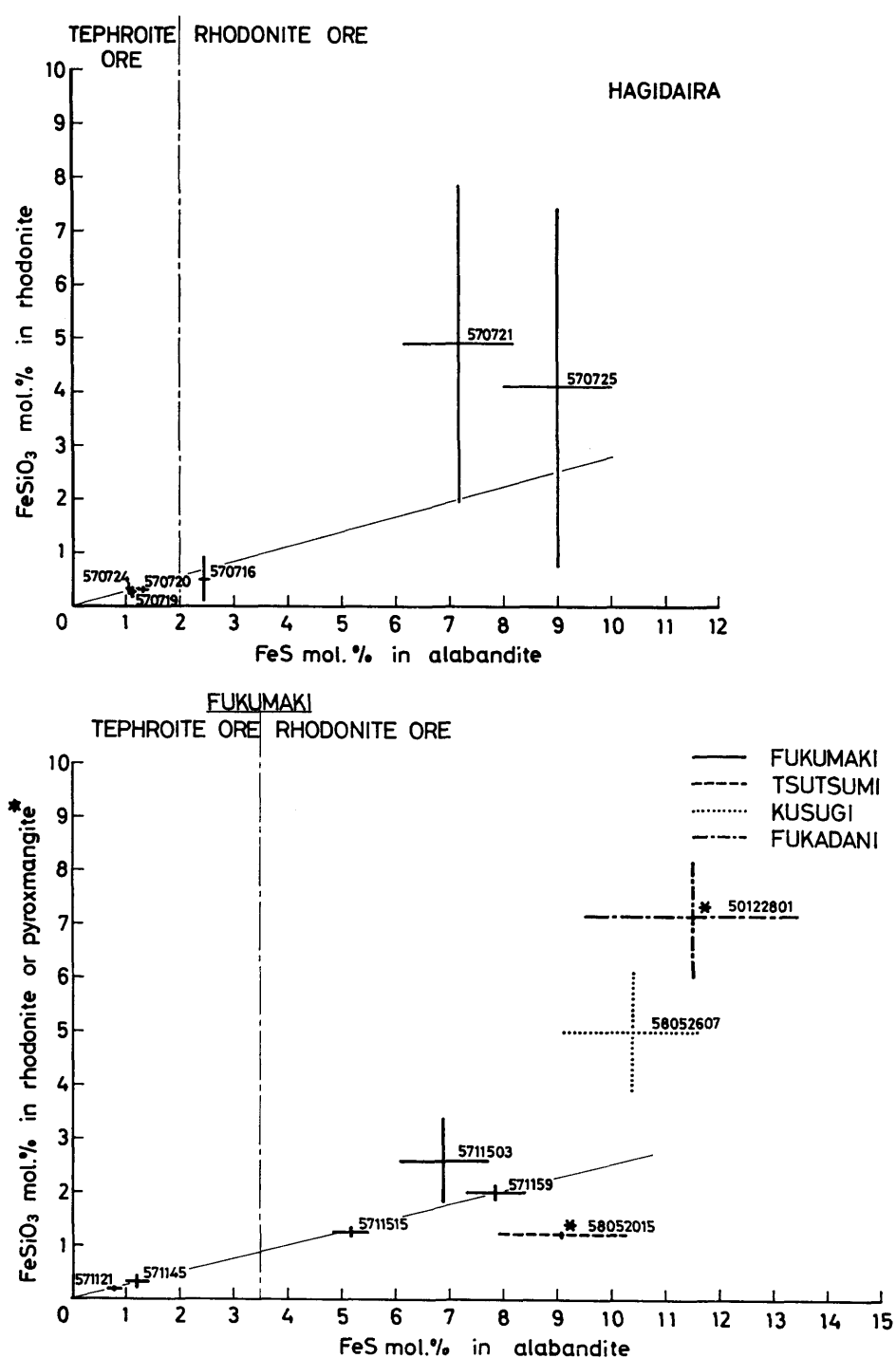


Fig. 7. Relation between iron content in rhodonite or pyroxmangite and that in alabandite.

a (upper): for Hagidaira mine,

b (lower): for Fukumaki, Tsutsumi, Kusugi, and Fukadani mines.

alabandite, but the most abundant and common minerals are rhodonite (or pyroxmangite), tephroite, and Mn-humites (allegghanyite and sonolite). These minerals can be divided into two pairs of rhodonite and pyroxmangite, and tephroite and Mn-humites by the compositional relations to alabandite as shown in Table 3. Relationship between the iron content in alabandite and that in the coexisting silicate minerals is considered for each pair as follows.

The samples examined amount to thirty-one in all, that is, Hanawa (570733), Shōwa (570708, 570706, 570704, 570707, 570709), Hagidaira (570728, 570730, 570719, 570720, 570724, 570716, 570721, 570725), Fukadani (50122801), Fukumaki (5711516, 5700521, 571121, 571193, 571145, 5711109(c), 5711505, 571118, 571148, 5711109(a), 5711128(a), 5711515, 5711503, 571159), Kusugi (58052607), and Tsutsumi (58052015). The chemical analyses of rhodonite, pyroxmangite, tephroite, allegghanyite, and sonolite are shown in Appendix I-D, -E, -F, -G, and -H, respectively.

Rhodonite and pyroxmangite

The relations between the FeSiO_3 content in rhodonite and pyroxmangite and the FeS content in alabandite is shown in Figure 7. The samples from Hagidaira and Fukumaki can be divided into two groups by the FeS content of alabandite, namely 2 mol.% and 3.5 mol.%. The iron-rich alabandite occurs in the rhodonite ore, and the iron-poor alabandite in the tephroite ore. The samples of Tsutsumi, Kusugi, and Fukadani mines consist of the rhodonite or pyroxmangite ore. In each case, the FeSiO_3 content in the pyroxenoids increases in proportion to the iron content in alabandite. But when FeS exceeds 6 or 7 mol.%, the FeSiO_3 content increases very rapidly and the variation of the iron content in the pyroxenoids within the same sample also becomes larger. Because alabandite exsolved an excess iron content as pyrrhotite. The difference between the iron content in rhodonite and pyroxmangite cannot be established clearly.

From these facts, it is pointed out that the iron content in the ores increases toward the rhodonite ore. Furthermore, the tendency becomes even greater as the amount of the iron sulfides increases when alabandite has higher FeS content (Table 3).

Tephroite and Mn-humites (allegghanyite and sonolite)

The relation between the iron content in tephroite and Mn-humites and that in alabandite is shown in Figure 8. The boundary values of FeS content in alabandite accompanied with rhodonite and tephroite ores in the Hagidaira and Fukumaki mines are the same as in Figure 7. The alabandite in the Shōwa and Hanawa mines is associated with rhodochrosite ore and that in the Tsutsumi mine is with pyroxmangite ore. The partition of iron between Mn-humites and alabandite leans slightly toward alabandite compared to that between tephroite and alabandite. However, it is considerably toward the silicates compared to that between pyroxenoids and alabandite. It is noteworthy that the relation given in Figure 8 shows a very clear linearity in comparison with the others.

Generally, the Mn-humites form solid solutions with wide range of iron content, as suggested from an example of low grade manganese ore from

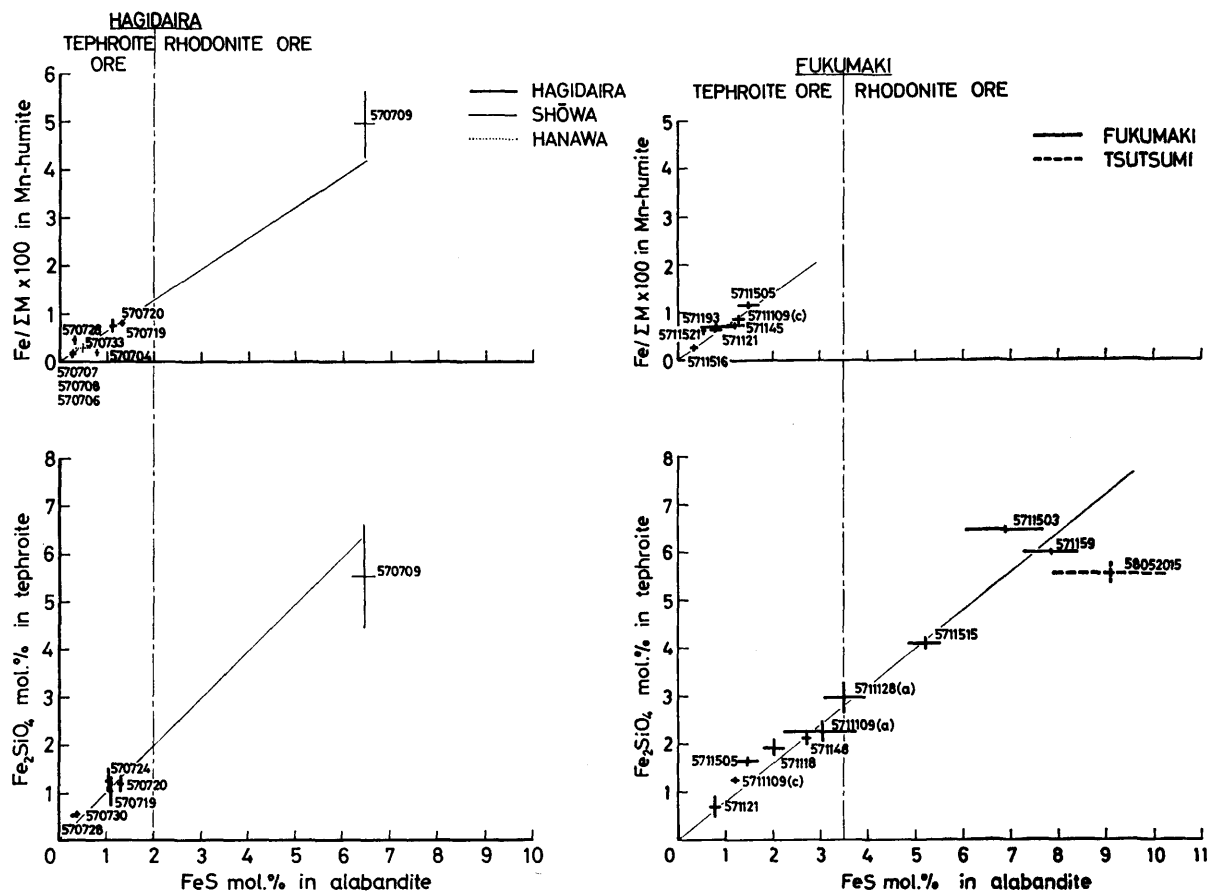


Fig. 8. Relation between iron content in tephroite or Mn-humites (alleganyite and sonolite) and that in alabandite.
 a (left): for Hagidaira, Shōwa, and Hanawa mines, b (right): for Fukumaki and Tsutsumi mines.

Shōwa (570709) where the amount of iron in the Mn-humite is very high and is nearly equal to that in the tephroite. But the Mn-humites are usually associated with high grade manganese ores such as manganese oxides, rhodochrosite, and tephroite, and the iron content is usually low. This may be due to the lack of iron when Mn-humites were formed.

In these cases of tephroite and Mn-humites, the same tendency is recognized again as the iron increases toward the rhodonite end from the tephroite side. Even when the difference of partition of iron in the rhodonite-alabandite and tephroite-alabandite pairs is considered, the tendency is still observed judging from the results in Figure 7 and Figure 8.

The fact that alabandite and associated manganese silicates have close correlation with respect to at least iron content indicates that these minerals have been formed intimately and simultaneously. Moreover it is most probable that the iron content of alabandite is mostly controlled by the partition coefficients of iron in relation to the associated major manganese silicates.

D. Manganese carbonates

As the manganese carbonates are the most common minerals associated with alabandite, the chemical composition and paragenesis of these minerals were also considered.

Rhodochrosite

The samples examined amount to twenty-seven in all, they are, Inakuraishi (R.C.), Hanawa (570733), Shōwa (570708, 570706, 570704, 570707, 570709), Hijikuzu (621095), Hagidaira (570730, 570719, 570720, 570724, 570716, 570721, 570725), Fukadani (50122801), Fukumaki (5711516, 5711521, 571121, 571193, 571145, 571119(c), 5711505, 571118, 571148, 571159), and Tsutsumi (58052015).

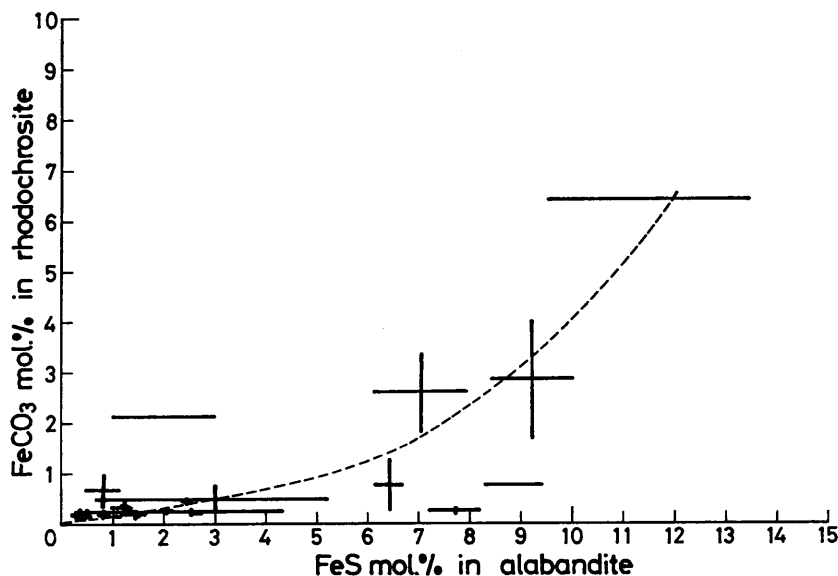


Fig. 9. Relation between iron content in rhodochrosite and that in alabandite.

The chemical analyses of manganese carbonates are shown in Appendix I-I. Their composition mostly converges into the rhodochrosite end member.

The relation between the iron content in rhodochrosite and that in alabandite

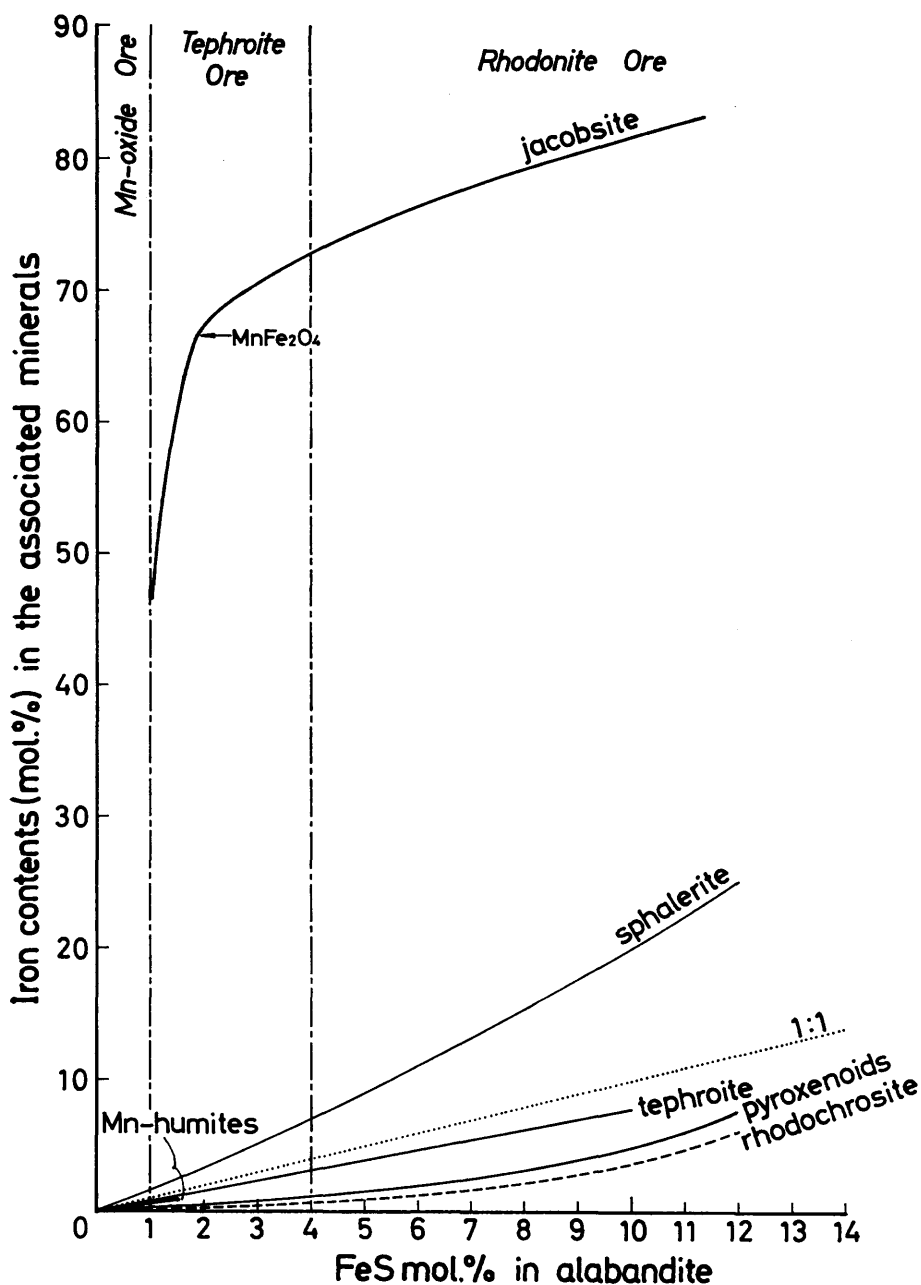


Fig. 10. Summary of the relations of iron content in alabandite versus that in sphalerite, jacobsite, pyroxenoids (rhodonite and pyroxmangite), tephroite, Mn-humites (alleganyite and sonolite), and rhodochrosite.

is represented in Figure 9. The correlation is observed between the iron content in rhodochrosite and in alabandite although it is not as clear as in the case of manganese silicates. However, the FeCO_3 content of rhodochrosite in the manganese carbonates ore is mostly less than 1 mol.%, and it does not fluctuate as widely as the FeS content in the associated alabandite.

The carbonates, however, frequently show irregular variations in the modes of occurrence, paragenetic relations, and chemical composition. It probably is due to the fact that they are sensitive to the environment during retrogressive process. Hence the carbonate composition does not always reflect the formation environment where alabandite deposited.

E. Summary

The relationships between the iron content in alabandite and those in several associated minerals are summarized in Figure 10. Considering all the samples shown in Figure 3, the boundary value of the FeS content in alabandite between Mn-oxide and tephroite ores and that between tephroite and rhodonite ores are 1 and 4, respectively. The figure indicates the distribution ratios of the iron content in the associated minerals against alabandite. The ratio is conspicuous in the case of jacobsonite and followed by sphalerite, tephroite, Mn-humites (alleganyite and sonolite), pyroxenoids (rhodonite and pyroxmangite), and rhodochrosite in the descending order. As to jacobsonite, it is indicated by synthetic studies of ONO *et al.* (1971) that the higher the content of manganese in the $\text{Mn}_3\text{O}_4\text{-Fe}_3\text{O}_4$ system, the higher the oxygen pressure is maintained under the formation environment. Then, the iron content in other minerals could also have been influenced by the oxygen pressures which controlled the ratio Fe^{2+} to Fe^{3+} .

In the bedded-type deposits affected by thermal metamorphism, the FeS content in alabandite generally increases according to the associated minerals in the order of manganoite and/or hausmannite and rhodochrosite, tephroite, and pyroxenoids as shown in Table 3. Because these assemblages are regarded to have been formed as a product of skarnization reactions among manganese carbonates, quartz, and silicate minerals, it is probable that the FeS content in alabandite has increased from the center of ore bodies to the wall rocks side and the oxygen pressure decreased. The variation of the bulk iron content in an ore body could not be quantitatively determined, but it is considered that the peripheral part of the ore body is rich in iron as compared with the central part.

In the unmetamorphosed bedded-type deposits, the amount of alabandite and its iron content are relatively small and iron distribution in an ore body is estimated to be rather homogeneous.

In the vein-type deposits, rhodochrosite is the major manganese mineral associated with alabandite and the reaction between the solid phase and hydrothermal solutions predominates over that between the solid phases, thus the distribution relations of the iron content are generally obscure.

From these results, it is concluded that considerable amount of iron ac-

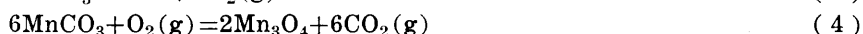
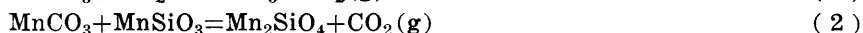
accompanied with sulfur was surely introduced from the wall rocks into the ore body under thermal metamorphism.

VII. Genetic environment of alabandite

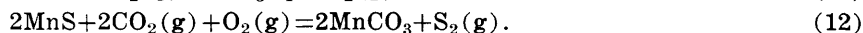
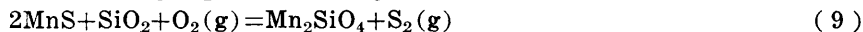
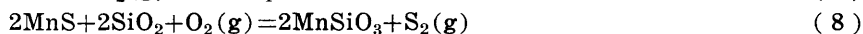
Although the modes of occurrence, paragenetic relations, and chemical composition of alabandite and several associated minerals are described above, it is still difficult to discuss the problems related to the physicochemical conditions and processes by which alabandite has formed, because it is intimately connected with the ore geneses involving the whole manganese deposits and also because the available synthetic experimental results and the thermochemical data are restricted to a few manganese minerals and moreover the laboratory data on natural assemblages are insufficient to quantify the complicated phase relations in nature.

Here, the author intends to discuss the genetic environment of alabandite by using chemical reactions within the Mn-S-C-O-Si system. The temperature range of interest is presumed to be 200–600°C and the total pressure is 1 bar in almost all cases. In reactions with gas phases in the equilibrium state higher pressures occur, but as the discussion is in the order of magnitude, the effects based on the difference of the total pressures and the addition of the other elements are neglected.

The next six equations are accepted as the principal reactions:



Then the reactions involving alabandite are expressed as follows:



In order to represent these reactions on a temperature- f_{O_2} diagram, the value of f_{CO_2} from the equations (1) to (3) and that of f_{S_2} from pyrrhotite-pyrite equilibrium are used. These values are likely to be within the range which alabandite-bearing manganese deposits were formed in nature. The equilibrium constants determined experimentally by CANDIA *et al.* (1975) and HUEBNER (1969) are used for the equations (1), (2), and (3) (Figure 11). Compiled data by BARTON and TOULMIN (1979) are applied to the pyrrhotite-pyrite reaction. FRENCH and EUGSTER (1965), HUEBNER and SATO (1970), and HOLLAND (1965) are adopted for the equations (5), (6), and (7), respectively.

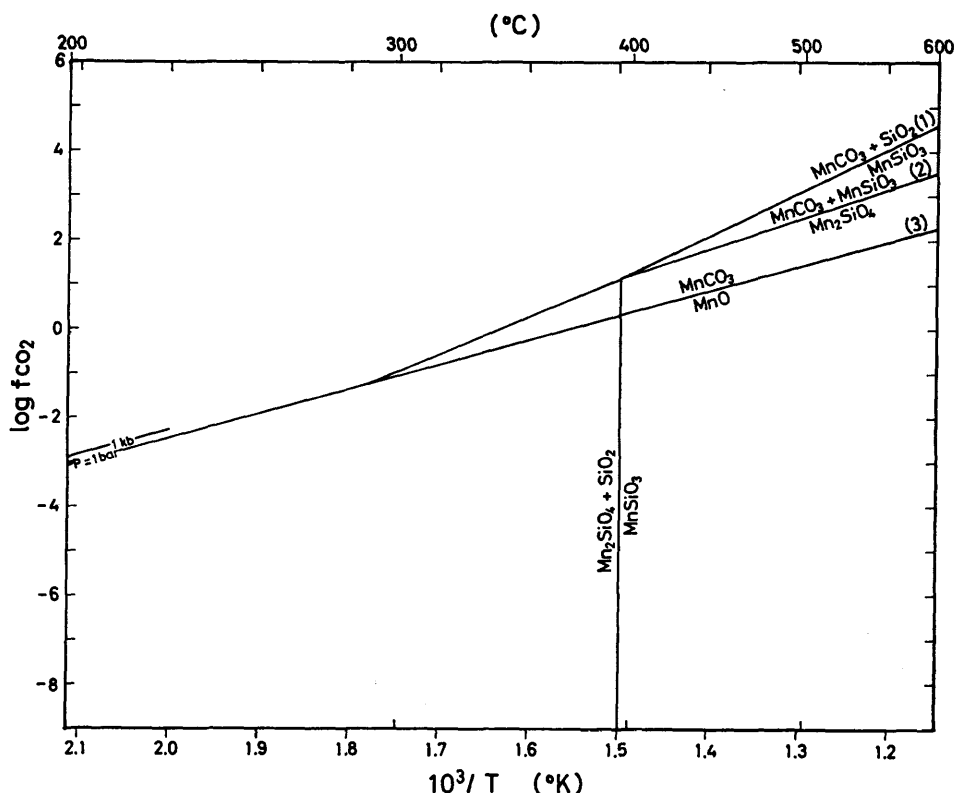


Fig. 11. Fugacity of CO_2 -temperature diagram for the reactions of (1) $\text{MnCO}_3 + \text{SiO}_2 = \text{MnSiO}_3 + \text{CO}_2$ (by CANDIA *et al.*, 1975), (2) $\text{MnCO}_3 + \text{MnSiO}_3 = \text{Mn}_2\text{SiO}_4 + \text{CO}_2$ (by CANDIA *et al.*, 1975), and (3) $\text{MnCO}_3 = \text{MnO} + \text{CO}_2$ (by HUEBNER, 1969).

Equilibrium constants for the other equations were calculated by using the thermochemical data presented by ROBIE *et al.* (1978).

The above equations and other several reactions of interest are plotted on a $\log f_{\text{O}_2} - 1/T$ ($^{\circ}\text{K}$) diagram as shown in Figure 12. In the figure, the upper boundary of alabandite stability field is controlled by the equation (7) and the lower limit is probably by equations (8) and/or (9). Other reactions involving alabandite are within this range. As alabandite stability coincides fundamentally with manganosite-hausmannite equilibrium (6) which is commonly found in nature, it is fully understood that alabandite should occur extensively in manganese deposits.

The modes of occurrence of alabandite are divided into three types as shown in Table 3. The difference of these occurrences will be considered from the relations given in Figure 12.

In the vein-type deposits, the alabandite stability is principally controlled by equations (1), (8), and (12). The f_{S_2} is assumed to be slightly higher than that of the pyrrhotite-pyrite equilibrium, and the f_{CO_2} considerably higher than that of the equation (1). Therefore, the curves of equations (8) and (12), shown in Figure 12, are depicted to the higher side of f_{O_2} . Moreover, the

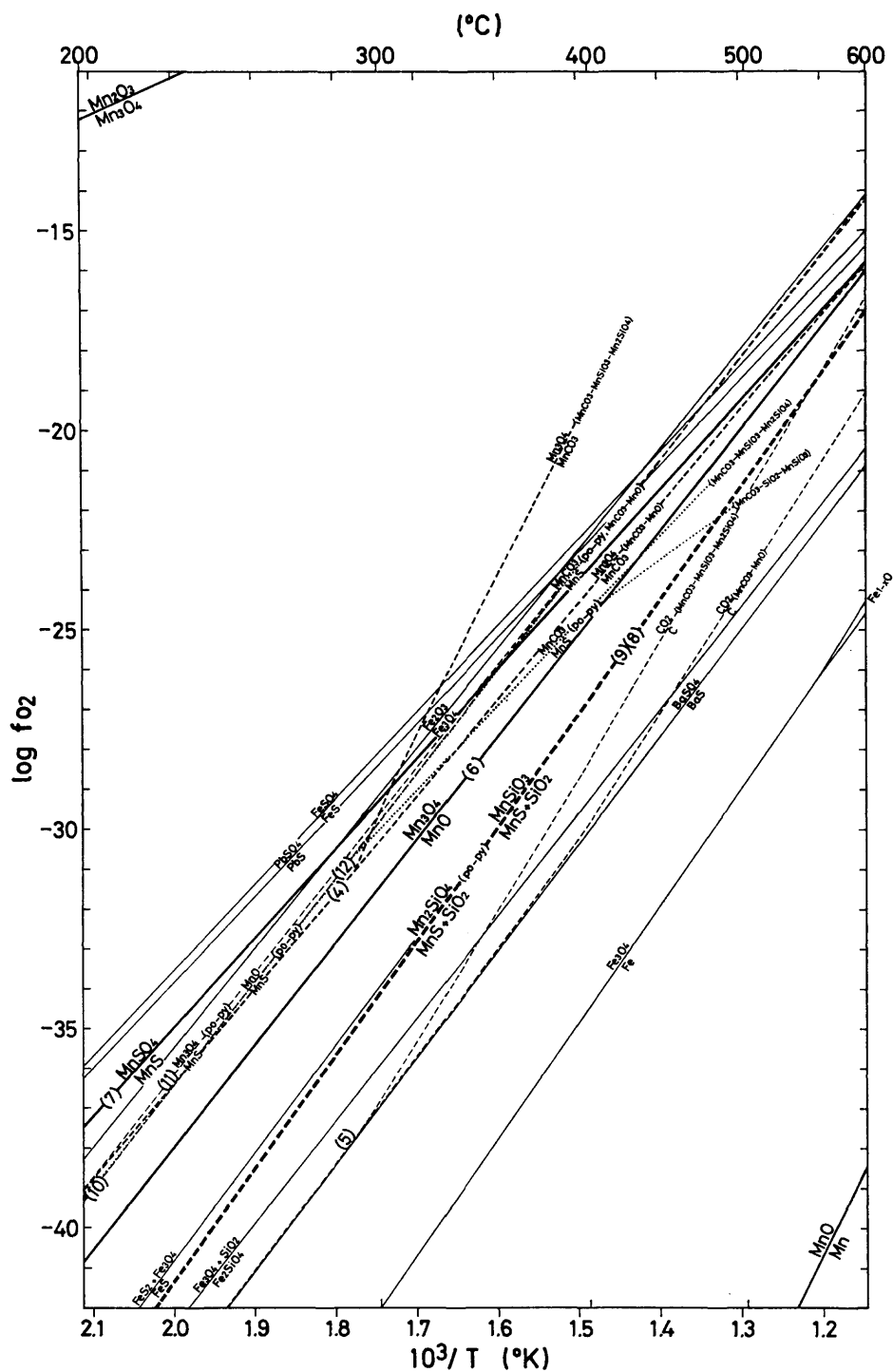


Fig. 12. Fugacity of O_2 -temperature diagram for the available reactions of Mn-S-O-C-Si system.

equation (12) is inferred to shift toward lower side of fo_2 . According to the experiments on fluid inclusions and measurements of FeS content in sphalerite and associated minerals (*e.g.*, ENJOJI and TAKENOUCHI, 1976), it seems that the fo_2 generally enters the field between the reactions (7) and (8) or (9) in the range 200–300°C. But in the more strict sense, the ore solution chemistry including the parameter of pH and so on should be considered because the solution played an important role in this case.

In the unmetamorphosed bedded-type deposits, if the fco_2 is controlled by the equations (2) and (3) and if hausmannite is present, the fo_2 will be near the upper boundary of the equation (4). From the equation (12), the increase of fco_2 is accompanied with the decrease of fo_2 at constant fs_2 , and if the fs_2 is equivalent to that of the pyrrhotite-pyrite equilibrium, the rhodochrosite+alabandite assemblage is stable in the field between equations (6) and (7). Because these deposits are generally composed mainly of rhodochrosite, the minor alabandite is most probably formed under the conditions of the equation (12).

In the metamorphosed bedded-type deposits, the predominant reactions in the manganosite and/or hausmannite-rhodochrosite ores can be regarded as the same as in the case of unmetamorphosed deposits, although the ranges of the formation temperatures are different. But in the tephroite and the rhodonite and/or pyroxmangite ores, the fco_2 is controlled by equations (1) and (2), and equations (8) and (9) predominate over the equation (12). The variations of the FeS content in alabandite cannot be interpreted by reactions given in Figure 12, because the small changes of the fs_2 should cause sensitive fluctuation of FeS content in alabandite and such sensitive changes cannot be handled in this discussion. But if the fs_2 varies in proportion to the fo_2 of equations (8)–(11), it is very likely that the fs_2 decreases together with the fo_2 , as the fco_2 increases generally from the value fixed by the equation (3) to the value by the equation (1). From the results, it is concluded that alabandite exhibits high ability to seize the FeS in the low grade manganese ore.

It is also concluded that two factors played important roles in the formation of alabandite-bearing ores in the manganese deposits: 1) the supply of iron to the peripheral part of a ore body, and 2) the difference in distribution ratios of the iron content between tephroite/alabandite and pyroxenoid/alabandite.

VIII. Concluding remarks

The results of the present study show that the paragenetic relations, chemical composition, and genetic environment of alabandite-bearing ores in the manganese deposits of Japan can be summarized as follows:

1) The paragenetic relations and chemical composition of alabandite are largely divided into three types by the differences in their modes of occurrence.

(i) *Tertiary vein-type deposits* Alabandite locally occurs as coarse grains, whose composition is generally heterogeneous with FeS content of 0.6 to 5.8 mol.%. No exsolution products are found in the minerals. The associated minerals consist mainly of rhodochrosite, pyrite, and quartz, and partly rhodonite.

(ii) *Paleozoic to Mesozoic, unmetamorphosed bedded-type deposits* Small amount of alabandite occurs dispersed in the deposits. It is fine-grained, composition is comparatively homogeneous within one grain, and the range of FeS is 0.2 to 6.6 mol.%. There is no exsolved mineral in alabandite. The associated minerals are mainly rhodochrosite accompanied with many kinds of manganese oxides and silicates, but very rarely with iron sulfides.

(iii) *Paleozoic to Mesozoic, thermally metamorphosed bedded-type deposits* Alabandite is abundant and widespread as medium to coarse grains in the deposits. Composition is quite homogeneous within one grain. The FeS content of alabandite ranges from 0.3 to 13.5 mol.%. It frequently contains pyrrhotite as exsolution products. The associated minerals consist of tephroite, rhodonite, and many kinds of the other manganese silicates, oxides, and carbonates. Abundant pyrrhotite and pyrite also coexist with alabandite.

2) In the above bedded-type deposits, there is a close correlation between the FeS content of alabandite and the kinds of the associated minerals. Namely, the FeS content in alabandite associated with hausmannite (including manganosite and jacobsonite) is less than 2 mol.%, tephroite less than 4 mol.%, and rhodonite (including pyroxmangite) less than 13.5 mol.%. In the highly metamorphosed deposits, FeS content of alabandite generally increases from the central to the peripheral parts.

3) As to the localization of alabandite occurrence by deposit types and also variation of the FeS content in alabandite, it is explained not only by the differences in the distribution ratios of the iron between alabandite and the associated manganese oxides (particularly, jacobsonite) and silicates (especially, tephroite, alleghanyite, sonolite, rhodonite, and pyroxmangite) but also by the introduction of iron accompanied with sulfur into the ore bodies during thermal metamorphism.

4) The stability field of alabandite can be calculated by using the selected principal reactions. It coincides approximately with the stability field of manganosite-hausmannite assemblage within the temperature range of deposit formation. This implies that alabandite occurs under wide range of physico-chemical conditions.

5) The FeS content in all alabandites analysed in this study ranges from 0.2 to 13.5 mol.%. Formation temperature can be calculated from the maximum FeS content to be about 350°C by using the alabandite geothermometer of SUGAKI and KITAKAZE (1972). But this indicates the temperature when the exsolution was completed during the later cooling period. The reaction rate of alabandite is considered to be relatively rapid. Therefore, the FeS content in alabandite in nature do not exceeded 13.5 mol.% to a large degree.

Acknowledgements

The writer is much indebted to Professor Fumitoshi HIROWATARI, Kyushu University, for his continuing guidance and encouragement, and furthermore for permitting him to use many samples. He expresses his sincere gratitude

to Dr. Nobutaka SHIMADA, Kyushu University, for helpful suggestions and critical reading of the manuscript. He is also grateful to Professor Haruo SHIROZU and Dr. Yoshikazu AOKI, Kyushu University, for informative discussions and valuable advice.

He would like to thank to Dr. Hiroharu MATSUEDA, Akita University, for providing the valuable samples from the Nodatamagawa and Yamada mines. Thanks are also due to Mr. Yoshinobu MOTOMURA, Kyushu University, for many helpful suggestions during the course of this work. Mrs. Hidemi AKAMINE, Kyushu University, kindly assisted the author in microprobe work.

References cited

- BARTON, P. B., Jr. and SKINNER, B. J. (1979): Sulfide mineral stabilities. In BARNES, H. L. 2nd ed., *Geochemistry of hydrothermal ore deposits*, Wiley-Interscience, New York, 278-403.
- BILTZ, W. and WIECHMANN, F. (1936): Zum System Mangan/Schwefel: Abbau und Synthese des Hauerits (MnS_2). *Z. anorg. u. allg. Chem.*, **228**, 268-274.
- CANDIA, M. A. F., PETERS, Tj. and VALARELLI, J. V. (1975): The experimental investigation of the reactions $\text{MnCO}_3 + \text{SiO}_2 = \text{MnSiO}_3 + \text{CO}_2$ and $\text{MnSiO}_3 + \text{MnCO}_3 = \text{Mn}_2\text{SiO}_4 + \text{CO}_2$ in $\text{CO}_2/\text{H}_2\text{O}$ gasmixtures at a total pressure of 500 bars. *Contrib. Mineral. Petrol.*, **52**, 261-266.
- ENJOJI, M. and TAKENOUCHI, S. (1976): Present and future researches of fluid inclusions from vein-type deposits (in Japanese with English abstract). *Mining Geol., Special Issue* (7), 85-100.
- FRENCH, B. M. and EUGSTER, H. P. (1965): Experimental control of oxygen fugacities by graphite-gas equilibrium. *J. Geophys. Res.*, **70**, 1529-1539.
- FUKUOKA, M. and HIROWATARI, F. (1980a): On minerals in the system Ni-Co-As-S from the bedded manganese ore deposits in the eastern part of Yamaguchi Prefecture: on the chemical compositions of gersdorffite-cobaltite solid solution (in Japanese with English abstract). *Sci. Rept., Dept. Geol., Kyushu Univ.*, **13**, (2), 239-249.
- and ——— (1980b): Chemical compositions of jacobssites from the bedded manganese ore deposits (in Japanese with English abstract). *Jour. Mineral. Soc. Japan*, **14**, *Special Issue* (3), 39-53.
- and ——— (1981): Manganese content of sphalerite from the manganese deposits in Japan (in Japanese with English abstract). *Sci. Rept., Dept. Geol., Kyushu Univ.*, **14**, (1), 1-12.
- HANSEN, M. and ANDERKO, K. (1958): *Constitution of binary alloys*, 1305 p, McGraw-Hill, New York.
- HARADA, Z. (1954a): Alabandite from the Inakuraishi mine, Siribesi Province, Hokkaido (in Japanese). *Hoku-chi-yoho*, **26**, 24.
- (1954b): Alabandite from the Tamamori mine, Siribesi Province, Hokkaido (in Japanese). *Hoku-chi-yoho*, **26**, 24.
- (1954c): On twin crystals of alabandite from the Inakuraishi mine, Siribesi Province, Hokkaido (in Japanese). *Jour. Mineral. Soc. Japan*, **1**, (6), 433-434.
- HATAE, N., SHIROZU, H. and MOMOI, H. (1965): Manganese deposits in Amami-oshima district (in Japanese). *Domestic Iron Resource Survey, MITI*, (3), 224-236.
- HATTORI, T. and HARADA, H. (1969): On the manganese silicate deposits of Furumiya mine in Ehime Prefecture—Report of the manganese silicate deposits in Japan (2)—(in Japanese with English abstract). *Bull. Geol. Surv. Japan*, **11**, (7), 443-450.
- HAYASHI, S. and IGARASHI, T. (1962): Report on the radiometric survey in Seta-gun,

- Gumma Prefecture (in Japanese with English abstract). *Bull. Geol. Surv. Japan*, **13**, (7), 573-582.
- HEWETT, D. F. and ROVE, O. N. (1930): Occurrence and relations of alabandite. *Econ. Geol.*, **25**, 36-56.
- HIROKAWA, O. (Chief ed.) (1978): *Geological map of Japan, 1:1,000,000* (2nd edition), Geol. Surv. Japan.
- HIROWATARI, F. (1961): Minerals and their paragenetic relations of the manganese deposits of Fukumaki mine, Yamaguchi Prefecture (in Japanese with English abstract). *Bull. Geol. Surv. Japan*, **12**, (8), 565-572.
- (1964): On some manganese garnets from the manganese ore deposits of Japan (in Japanese with English abstract). *Sci. Rept., Dept. Geol., Kyushu Univ.*, **7**, (1), 113-119.
- and TAKEDA, H. (1962a): On the manganese ore deposits in the Watarase river district, Gumma Prefecture—Report of the manganese silicate deposits in Japan (4)—(in Japanese with English abstract). *Bull. Geol. Surv. Japan*, **13**, (5), 437-452.
- and ——— (1962b): On the manganese ore deposits in the Kaso, Hikoma and Hishimura districts, Tochigi Prefecture—Report of the manganese silicate deposits in Japan (5)—(in Japanese with English abstract). *Bull. Geol. Surv. Japan*, **13**, (8), 683-708.
- HOLLAND, H. D. (1965): Some applications of thermochemical data to problems of ore deposits II. Mineral assemblages and the compositions of ore-forming fluids. *Econ. Geol.*, **60**, 1101-1166.
- HUEBNER, J. S. (1969): Stability relations of rhodochrosite in the system manganese-carbon-oxygen. *Am. Mineral.*, **54**, 457-481.
- and SATO, M. (1970): The oxygen fugacity-temperature relationships of manganese oxide and nickel oxide buffers. *Am. Mineral.*, **55**, 934-952.
- ISHIDA, H. (1976): *Phase equilibrium study in the Mn-Fe-S system* (in Japanese with English abstract). Unpub. M. Eng. thesis, Yamaguchi Univ.
- , SUGAKI, A. SHIMA, H. and KITAKAZE, A. (1977): Phase equilibrium study in the Mn-Fe-S system (II) (abst.) (in Japanese). *Joint Symposium, Niigata*, C25.
- ITO, T. and SAKURAI, K. (1947): *Wada's minerals of Japan* (3rd edition) (in Japanese), Mineral. Inst., Univ. Tokyo, Tokyo.
- KATO, A. and MATSUBARA, S. (1980): Manganese borate minerals from Japan (in Japanese with English abstract). *Jour. Mineral. Soc. Japan*, **14**, Special Issue (3), 86-97.
- , NAKAMA, T. and MATSUMOTO, M. (1965): Manganese deposits in Aso and Kamitsuga districts (I) (in Japanese). *Domestic Iron Resource Survey, MITI*, (3), 146-154.
- LEE, D. E. (1955): *Mineralogy of some Japanese manganese ores*, 64 p, Stanford Univ., California.
- MATSUBARA, S. and KATO, A. (1977): Unknown Ba-V-silicates from Mogurazawa mine in Kiryu City (abst.) (in Japanese). *Annual Meet. Mineral. Soc. Japan, Tokyo*, A01.
- MEHMED, F. and HARALDSEN, H. (1938): Das magnetische Verhalten der allotropen Modifikationen des Mangan (II)-Sulfids. *Z. anorg. u. allg. Chem.*, **235**, 193æ200.
- MIYAMOTO, H., OTSU, H. and KAWANO, T. (1962): On the manganese silicates ore deposits in Taguchi district, Aichi Prefecture—Report of the manganese silicate deposits in Japan (3)—(in Japanese with English abstract). *Bull. Geol. Surv. Japan*, **13**, (5), 424-436.
- , TAKASE, H. and MARUYAMA, S. (1954): Report on manganese deposits at Kanuma district, Tochigi Prefecture (in Japanese with English abstract). *Bull. Geol. Surv. Japan*, **5**, (4), 163-182.
- NAMBU, M. (1965): *Report of minerals from Iwate Prefecture* (in Japanese), 252 p,

- Iwate Prefecture.
- and TANIDA, K. (1964): Oxidation of the manganese ore deposits of Taki mine, Iwate Prefecture—With special reference to the formation of amorphous manganese dioxide mineral—(in Japanese with English abstract). *Jour. Japan. Assoc. Mineral. Petrol. Econ. Geol.*, **51**, (6), 223–232.
- , ———, KITAMURA, T. and KUMAGAI, S. (1976): Constituent minerals in the manganese ore deposits of Hijikuzu mine, Iwate Prefecture (abst.) (in Japanese). *Joint Symposium, Kagoshima*, B46.
- , ———, OIKAWA, S., KUMAGAI, S. and NASUKAWA, S. (1973): *Manganese deposits in the Kitakami mountains II* (in Japanese), 85 p, Iwate Prefecture.
- ONO, K., UEDA, T., OZAKI, T., UEDA, Y., YAMAGUCHI, A. and MORIYAMA, J. (1971): Thermodynamic study of the iron-manganese-oxygen system (in Japanese with English abstract). *Nippon Kinzoku Gakkaishi*, **35**, (8), 757–763.
- ROBIE, R. A., HEMINGWAY, B. S. and FISHER, J. R. (1978): Thermodynamic properties of minerals and related substances at 298.15K and 1 bar (10^5 pascals) pressure and at higher temperatures, 456 p, *U. S. Geol. Survey Bull.*, **1452**.
- SAITO, M., BAMBA, T., SAWA, T., NARITA, E., IGARASHI, T., YAMADA, K. and SATOH, H. (1967): *Metallic and non-metallic mineral deposits of Hokkaido, Japan* (in Japanese with English abstract), 575 p, Geol. Surv. Japan.
- SAKURAI, K. (1956): Localities of sphalerite showing crystal forms (in Japanese). *Jour. Mineral. Soc. Japan*, **2**, 385.
- SATO, A., FUKUDA, K. and WADA, T. (1957): On the manganese deposits and its prospecting of Nodatamagawa mine, Iwate Prefecture (1), (2) (in Japanese with English abstract). *Mining Geol.*, **7**, (23), (24), 13–21, 98–103.
- SCHNAASE, H. (1933): Kristallstruktur der Mangansulfide und ihrer Mischkristalle mit Zinksulfid und Cadmiumsulfid. *Z. physik. Chem. Abt.*, **20**, 89–117.
- SCOTT, S. D. and BARNES, H. L. (1971): Sphalerite geothermometry and geobarometry. *Econ. Geol.*, **66**, 653–669.
- SHINODA, M., SAKAI, T., KOONO, J. and KIKUCHI, H. (1974): Geology of the Ooe-Inakuraishi mine, with special reference to the vein system (in Japanese with English abstract). *Mining Geol.*, **24**, (2), 119–128.
- SHIBATA, Z. (1928): The equilibrium diagram of the iron sulphide-manganese sulphide system. *Tech. Rep. Tohoku Imp. Univ.*, **6**, 279–289.
- SHIROZU, H. (1949): On the manganese deposits of the Ioi mine, Shiga Prefecture, with special reference to hausmannite (in Japanese with English abstract). *Jour. Geol. Soc. Japan*, **55**, (646), 77–83.
- SKINNER, B. J. and LUCE, F. D. (1971): Solid solutions of the type (Ca, Mg, Mn, Fe)-S and their use as geothermometers for the enstatite chondrites. *Am. Mineral.*, **56**, 1269–1296.
- SUGAKI, A. and KITAKAZE, A. (1972): Chemical composition of synthetic alabandite solid solution and its phase relations in the system Fe-Mn-S. *Proc. 6th Int. Conf. X-ray Opt. Microanal.*, 755–760.
- SUZAKI, Y., URASHIMA, Y. and HAYAKAWA, A. (1969): On the ore of the Yūbaridake manganese mine, Hokkaido (in Japanese with English abstract). *Mining Geol.*, **19**, (96), 147–158.
- TOZUKA, Y. and KOBAYASHI, S. (1964): Manganese deposits in Ashio district (in Japanese). *Domestic Iron Resource Survey, MITI*, (2), 190–195.
- WATANABE, M. (1939): The pseudomorph of barite and the mode of occurrence of alabandite in silver and manganese ores from Mori mine (in Japanese). *Jour. Japan. Assoc. Mineral. Petrol. Econ. Geol.*, **22**, 136–147.
- WATANABE, T. (1959): The minerals of the Noda-Tamagawa mine, Iwaté Prefecture, Japan I. Notes on geology and parageneses of minerals. *Mineral. Jour.*, **2**, (6), 408–421.
- and KIMURA, M. (1954): The mode of occurrence and paragenesis of alabandite

- (abst.) (in Japanese). *Mining Geol.*, 4, 46.
- , YUI, S. and KATO, A. (1970): Bedded manganese deposits in Japan, a review. In TATSUMI, T. ed., *Volcanism and ore genesis*, Univ. Tokyo, Tokyo, 119–142.
- WYCKOFF, R. W. G. (1921): Art. XVII.—The structure of alabandite (MnS). *Am. Jour. Sci.*, Fifth Series, II, 239–249.
- YASUDA, M. (1965): Manganese deposits in Ōidani district (in Japanese). *Domestic Iron Resource Survey, MITI*, (3), 203–205.
- YOSHIE, H. and HIROWATARI, F. (1978): The modes of occurrence and ore minerals in the manganese deposits of Hamayokogawa mine (abst.) (in Japanese). *Joint Symposium, Hiroshima*, B18.
- YOSHIMURA, T. (1937): Alabandite and rhodochrosite from Hokkaido (abst.) (in Japanese). *Jour. Geol. Soc. Japan*, 44, 559–560.
- (1967): Supplement to “Manganese ore deposits of Japan” Part I Manganese mineralization, minerals and ores (in Japanese with English abstract). *Sci. Rept., Dept. Geol., Kyushu Univ.*, 9, *Special Issue* (1), 1–485.
- (1969): Supplement to “Manganese ore deposits of Japan” Part II Manganese mines of Japan (in Japanese with English abstract). *Sci. Rept., Dept. Geol., Kyushu Univ.*, 9, *Special Issue* (2), 487–1004.
- and MOMOI, H. (1961): Dannemorite from Zomeki, Yamaguchi Prefecture, Japan (in Japanese with English abstract). *Sci. Rept., Dept. Geol., Kyushu Univ.*, 5, (3), 99–110.
- and ——— (1964): Withamite from the Yamanaka mine, Hyogo Prefecture (in Japanese with English abstract). *Sci. Rept., Dept. Geol., Kyushu Univ.*, 6, (3), 201–206.
- and YOSHINAGA, M. (1959): Helvite from Yagisawa mine, Nagano Prefecture (in Japanese). *Jour. Mineral. Soc. Japan*, 4, (1,2) 34–41.

Appendix I. Electron microprobe data.

A. Alabandite analyses

	wt. %				
	S	Mn	Fe	Total	FeS mol. %
<u>Inakuraishi</u>					
R.C.-A-1-1	36.91	59.41	2.80	99.12	4.43
-A-1-2	37.25	59.99	3.37	100.61	5.23
-A-2-1	37.26	59.58	3.13	99.97	4.91
-A-2-2	37.36	60.85	1.60	99.81	2.51
-A-2-3	36.83	60.30	1.75	98.88	2.78
-A-3-1	37.18	60.48	2.17	99.83	3.41
-A-3-2	37.11	59.51	2.92	99.54	4.61
-A-4-1	36.95	60.43	1.70	99.08	2.70
-A-4-2	36.85	60.62	1.67	99.14	2.65
-A-4-3	36.95	61.19	1.45	99.59	2.28
-1-2-1	37.99	62.86	0.50	101.35	0.78
-1-2-2	37.45	60.80	1.47	99.72	2.32
-1-2-3	37.10	60.89	1.54	99.53	2.42
-1-2-4	37.79	63.09	0.42	101.30	0.65
-1-4-1	37.99	62.76	0.56	101.31	0.86
-1-4-2	37.61	60.01	2.31	99.93	3.64
-2-2-6	37.05	59.74	1.67	98.46	2.64
-2-2-7	37.62	60.51	1.53	99.66	2.42
-2-2-10	37.73	60.55	1.75	100.03	2.74
-C-2-1-4	37.13	60.47	2.66	100.26	4.14
-C-2-4-4	36.47	60.36	1.64	98.47	2.60
-C-1-2-3	36.52	59.29	2.46	98.27	3.90
-C-1-2-4	36.40	59.57	2.37	98.34	3.74
-A-1-B-3	37.03	59.19	3.18	99.40	4.98
-C-3-1-4	37.37	62.15	1.32	100.84	2.04
<u>Mori</u>					
621080-A-1-1	37.67	62.52	1.05	101.24	1.63
-A-1-2	37.70	63.35	0.63	101.68	0.97
-A-1-3	37.87	62.94	0.80	101.61	1.23
-A-1-4	37.63	62.16	1.03	100.82	1.60
-A-1-5	37.76	61.40	2.22	101.38	3.44
-A-2-1	37.91	62.63	1.06	101.60	1.63
-A-2-2	37.74	61.52	1.73	100.99	2.69
-A-2-3	37.79	62.28	1.04	101.11	1.62
-A-2-4	37.67	62.04	1.72	101.43	2.65
-A-2-5	37.98	62.38	1.52	101.88	2.34
-A-3-1	37.46	61.45	1.21	100.12	1.90
-A-3-2	37.36	61.76	1.22	100.34	1.90
-A-3-3	37.64	62.74	0.79	101.17	1.22
-A-3-4	37.18	62.53	1.02	100.73	1.57
-A-3-5	37.34	61.61	1.11	100.06	1.74
-B-1-1	37.17	62.10	0.89	100.16	1.40
-B-1-3	37.17	61.97	1.08	100.22	1.69
-B-1-4	36.82	61.27	1.45	99.54	2.26
-B-1-5	37.26	62.13	1.04	100.43	1.62
-B-1-6	36.82	61.19	1.31	99.32	2.06
-B-2-1	37.17	60.79	2.06	100.02	3.23
-B-2-2	36.75	60.55	2.25	99.55	3.53
-B-2-3	37.04	60.85	2.08	99.97	3.26
-B-2-4	37.12	61.54	1.81	100.47	2.81
-B-2-5	36.85	60.63	2.18	99.66	3.41
-B-3-1	36.82	58.85	3.69	99.36	5.81

A-1

A. (continued)

	wt. %				
	S	Mn	Fe	Total	FeS mol. %
-B-3-2	36.90	59.18	3.70	99.78	5.79
-B-3-3	37.01	59.25	3.44	99.70	5.40
-B-3-4	37.06	59.75	3.57	100.38	5.55
-B-3-5	37.11	58.98	3.68	99.77	5.78
-B-3-6	37.12	59.71	3.53	100.36	5.50
-B-3-7	36.62	58.65	3.62	98.89	5.72
-B-3-8	36.46	59.12	3.67	99.25	5.75
-B-3-9	36.71	59.36	3.59	99.66	5.62
-B-3-10	37.35	60.22	3.61	101.18	5.58
<u>Yamanaka</u>					
A-1-1	37.95	61.65	2.27	101.87	3.49
-1-2	37.65	61.13	2.42	101.20	3.74
-2-1	37.42	61.24	2.67	101.33	4.12
-2-2	37.54	61.13	2.70	101.37	4.16
-3-1	37.45	61.07	2.83	101.35	4.36
-3-2	37.39	61.48	2.75	101.62	4.21
<u>Hanawa</u>					
570733-1-1	37.33	62.53	0.20	100.06	0.31
-1-2	37.89	63.38	0.21	101.48	0.33
-1-5	37.61	63.28	0.19	101.08	0.29
-4-3	35.90	61.74	0.38	98.02	0.59
-4-4	36.77	62.46	0.29	99.52	0.45
570739-2-1-2	36.96	59.29	3.46	99.71	5.42
-2-1-3	37.22	59.87	3.48	100.57	5.40
<u>Nakanoyama</u>					
570746-1-1	37.00	62.92	0.47	100.39	0.72
-1-2	37.09	63.73	0.47	101.29	0.72
-3-1	37.45	63.53	0.54	101.52	0.83
-4-1	37.24	63.12	0.63	100.99	0.98
-5-1	37.34	63.45	0.89	101.68	1.36
-5-2	37.31	62.89	0.83	101.03	1.28
-6-1	37.43	63.19	0.57	101.19	0.89
-6-2	37.35	63.11	0.52	100.98	0.81
<u>Rito</u>					
570741-2-1	37.25	63.76	0.32	101.33	0.49
-2-2	36.84	63.39	0.25	100.48	0.39
-2-3	37.07	63.28	0.27	100.62	0.41
-3-1	37.29	63.85	0.24	101.38	0.37
-3-2	37.34	63.41	0.29	101.04	0.44
-3-3	37.63	63.57	0.32	101.52	0.48
-4-1	37.55	63.24	0.30	101.09	0.46
-4-2	37.42	63.17	0.27	100.86	0.41
-4-3	37.03	63.87	0.22	101.12	0.34
-5-1	37.36	63.53	0.42	101.31	0.64
-5-2	37.30	63.68	0.31	101.29	0.47
-5-3	37.38	63.44	0.39	101.21	0.59
570742-1-1	38.33	63.93	0.21	102.47	0.32
-3-1	37.67	64.14	0.53	102.34	0.81
-3-2	37.77	64.31	0.69	102.77	1.05
570743-1-1	37.14	63.29	1.01	101.44	1.54
-1-2	37.34	62.48	1.25	101.07	1.93
-1-3	37.43	62.16	1.27	100.86	1.96
-1-4	37.22	63.04	1.10	101.36	1.68
-1-5	36.87	62.45	0.72	100.04	1.12
-2-1	37.42	62.72	1.08	101.22	1.66

A-2

A. (continued)

	wt. %				FeS mol. %
	S	Mn	Fe	Total	
-2-2	37.48	62.34	1.09	100.91	1.69
-2-3	37.41	62.64	1.15	101.20	1.77
-2-4	37.42	62.68	0.93	101.03	1.44
-2-5	37.16	62.84	0.76	100.76	1.18
<u>Showa</u>					
570708-2-1	35.84	63.49	0.18	99.51	0.27
-2-2	35.86	63.11	0.17	99.14	0.26
-3-1	36.42	63.73	0.17	100.32	0.25
-3-2	34.60	63.78	0.18	98.56	0.27
-4-1	36.06	63.62	0.17	99.85	0.26
-4-2	36.21	63.64	0.18	100.03	0.27
570706-1-1	37.30	63.25	0.14	100.69	0.21
-1-2	37.48	63.27	0.24	100.99	0.36
-1-3	36.81	63.50	0.23	100.54	0.35
-2-1	37.38	63.54	0.20	101.12	0.30
-2-2	37.27	63.26	0.21	100.74	0.32
-2-3	37.59	63.68	0.19	101.46	0.29
-3-1	36.99	63.44	0.17	100.60	0.26
-3-2	36.86	63.49	0.21	100.56	0.32
-3-3	37.07	63.51	0.24	100.82	0.37
570704-2-1	36.19	62.49	0.50	99.18	0.79
-2-3	36.46	62.31	0.51	99.28	0.81
570710-3	36.28	63.60	0.52	100.40	0.80
-5	36.38	63.44	0.60	100.42	0.92
570707-1-1	36.17	61.21	2.63	100.01	4.05
-1-2	36.14	60.91	2.72	99.77	4.21
-1-3	36.19	61.31	2.53	100.03	3.90
-1-7	35.92	61.12	2.83	99.87	4.35
-2-1	36.30	63.95	0.20	100.45	0.30
-2-2	36.29	64.02	0.16	100.47	0.24
-2-3	35.88	63.39	0.19	99.46	0.29
-2-4	36.30	64.22	0.20	100.72	0.30
-2-5	36.21	63.81	0.23	100.25	0.35
570709-1-1	38.28	59.09	4.03	101.40	6.28
-1-2	37.95	59.30	4.24	101.49	6.58
-1-3	38.43	59.06	3.95	101.44	6.17
-1-6	37.83	59.28	4.17	101.28	6.47
-1-7	37.22	59.00	3.98	100.20	6.22
-1-8	37.84	59.16	4.05	101.05	6.32
-1-9	37.98	58.56	4.07	100.61	6.40
-3-1	37.88	59.29	3.99	101.16	6.21
-3-2	37.63	58.15	4.11	99.89	6.49
-3-3	37.30	58.20	4.00	99.50	6.33
<u>Hamayokogawa</u>					
5208-1-1-1	37.24	63.26	0.15	100.65	0.23
-1-1-2	36.35	62.71	0.15	99.21	0.23
-1-2-1	36.97	63.47	0.23	100.67	0.35
-1-2-2	37.09	64.11	0.16	101.36	0.24
-1-2-3	37.25	63.33	0.18	100.76	0.27
-1-3-1	36.87	62.92	0.18	99.97	0.28
-1-3-2	37.26	63.22	0.18	100.66	0.27
-1-3-3	37.21	63.14	0.20	100.55	0.31
-2-2-2	37.77	63.44	0.16	101.37	0.24
-2-2-3	37.39	63.73	0.17	101.29	0.26
-2-3-1	36.79	64.23	0.20	101.22	0.30
5205-1-1-2	37.54	63.94	0.33	101.81	0.50

A-3

A. (continued)

	wt. %				FeS mol. %
	S	Mn	Fe	Total	
-1-3-1	38.18	61.74	0.18	100.10	0.29
-1-3-2	37.77	62.64	0.20	100.61	0.31
-1-3-3	37.73	62.30	0.18	100.21	0.28
-1-4-1	37.83	63.06	0.19	101.08	0.30
-1-4-2	38.44	63.03	0.22	101.69	0.34
-1-4-3	38.22	63.29	0.18	101.69	0.28
-2-1-1	37.34	63.72	0.20	101.26	0.30
-2-1-2	37.07	63.17	0.17	100.41	0.26
-2-1-3	37.92	63.87	0.16	101.95	0.24
-2-2-1	37.92	63.29	0.14	101.35	0.22
-2-2-2	37.96	63.66	0.15	101.77	0.22
-2-3-1	37.44	63.43	0.18	101.05	0.27
-2-3-2	37.69	63.32	0.18	101.19	0.27
-2-3-3	37.79	63.36	0.15	101.30	0.23
<u>Furumiya</u>					
5812108-B-1-1	37.37	63.49	0.13	100.99	0.20
-B-1-2	37.74	63.66	0.12	101.52	0.18
-B-2-1	37.78	63.75	0.11	101.64	0.17
-B-2-2	37.89	63.22	0.13	101.24	0.20
-B-3-1	37.55	63.35	0.12	101.02	0.18
-B-3-2	37.90	63.68	0.13	101.71	0.20
-D-1-1	37.44	63.07	0.30	100.81	0.47
-D-1-2	37.45	63.46	0.32	101.23	0.49
-D-1-3	37.22	63.44	0.36	101.02	0.55
-D-2-1	37.32	63.83	0.17	101.32	0.26
-D-2-2	37.56	63.74	0.16	101.46	0.24
-D-3-1	37.78	63.11	0.31	101.20	0.48
<u>Hijikuzu</u>					
621095-1-B-1-2	37.54	62.95	0.92	101.41	1.42
<u>Nodatamagawa</u>					
L12-G-1-1	36.96	62.07	1.77	100.80	2.73
-1-2	37.21	61.63	1.77	100.61	2.75
-2-1	37.04	61.67	1.83	100.54	2.84
-2-2	37.50	61.84	1.68	101.02	2.61
-3-2	36.98	61.76	1.79	100.53	2.77
S.Z.-1-1-1	36.91	61.31	2.01	100.23	3.12
-1-1-2	36.94	62.02	1.85	100.81	2.85
-1-2-1	37.32	61.06	2.10	100.48	3.27
-1-2-2	37.29	61.06	2.09	100.44	3.26
-1-3-1	37.20	61.97	1.56	100.73	2.42
-1-3-2	36.87	61.21	1.92	100.00	2.99
-2-2-1	36.55	60.48	2.16	99.19	3.39
V.C.-1-1-1	37.16	60.12	3.07	100.35	4.78
-1-1-2	37.20	60.07	3.48	100.75	5.38
-1-2-1	37.13	60.59	2.87	100.59	4.45
-1-2-2	37.01	61.68	2.74	101.43	4.19
-1-3-1	37.37	60.37	2.82	100.56	4.40
-1-3-2	36.84	61.09	2.90	100.83	4.46
-2-1-1	37.54	60.96	2.92	101.42	4.51
-2-1-2	36.99	60.42	2.89	100.30	4.50
-2-2-1	37.14	59.94	2.89	99.97	4.53
-2-2-2	37.41	60.24	2.87	100.52	4.48
L12-1-1-1	38.10	56.37	6.95	101.42	10.82
-1-2	38.28	57.35	5.93	101.56	9.24
-2-1	38.04	57.34	6.16	101.54	9.55
-2-2	37.86	57.32	6.48	101.66	10.01

A-4

A. (continued)

	wt. %				FeS mol. %
	S	Mn	Fe	Total	
-2-A	35.44	58.54	5.55	99.53	8.53
-3-1	37.43	56.95	7.13	101.51	10.97
-3-2	37.67	56.00	7.14	100.81	11.14
-2-1-A	37.79	55.41	7.89	101.09	12.28
-1-B	37.38	55.80	7.43	100.61	11.59
-2-1	37.54	55.85	7.24	100.63	11.31
-2-2	37.72	57.14	6.16	101.02	9.58
-2-A	37.91	56.73	6.71	101.35	10.43
-2-B	38.44	57.20	6.06	101.70	9.45
-3-B	37.59	61.92	1.84	101.35	2.84
V.O.-1-1-1	37.01	56.19	7.46	100.66	11.55
-1-1-2	37.54	56.02	7.39	100.95	11.48
-1-2-1	37.29	54.99	7.70	99.98	12.11
-1-2-2	37.34	55.38	7.25	99.97	11.41
-3-1-1	37.15	57.41	7.24	101.80	11.03
-3-1-2	37.18	56.47	7.26	100.91	11.23
<u>Kaso</u>					
28-2-1-1	37.52	63.68	0.28	101.48	0.42
-2-1-2	37.61	63.06	0.34	101.01	0.52
-2-2-1	37.67	63.75	0.34	101.76	0.51
-2-2-2	37.56	63.55	0.37	101.48	0.56
29-2-2-2	37.91	63.69	0.33	101.93	0.50
22-B-2-1-1	37.65	62.48	1.48	101.61	2.27
-2-1-2	37.51	62.61	1.47	101.59	2.27
-2-1-3	37.99	62.54	1.30	101.83	2.00
-2-2-1	36.81	62.46	1.06	100.33	1.64
-2-2-3	37.57	63.06	1.03	101.66	1.58
-2-3-1	37.46	62.41	1.23	101.10	1.90
-2-3-2	37.38	62.75	1.22	101.35	1.87
<u>Hagidaira</u>					
570728-1	36.58	63.74	0.19	100.51	0.28
-2	37.04	64.03	0.20	101.27	0.31
-3	36.49	63.62	0.19	100.30	0.29
570730-2	36.72	62.58	0.21	99.51	0.32
-3	36.35	61.71	0.26	98.32	0.41
-4	35.90	62.43	0.28	98.61	0.43
570717-1-1	36.30	63.17	0.33	99.80	0.51
-1-2	35.98	62.62	0.32	98.92	0.49
-1-3	36.13	62.63	0.32	99.08	0.49
-2-1	35.88	63.43	0.36	99.67	0.55
-2-2	36.70	62.56	0.37	99.63	0.57
570719-4-1	36.34	61.91	0.71	98.96	1.12
-4-2	36.36	61.78	0.68	98.82	1.08
-4-3	36.40	61.70	0.69	98.79	1.10
570720-2-1	36.74	61.94	0.80	99.48	1.26
-2-2	36.59	61.49	0.80	98.88	1.27
-2-3	36.66	62.12	0.87	99.65	1.37
570724-1	36.37	59.98	1.81	98.16	2.89
-2	37.51	60.50	1.88	99.89	2.97
-4	35.69	63.12	0.63	99.44	0.98
-5	36.83	62.55	0.69	100.07	1.08
570718-1-1	36.69	61.35	1.18	99.22	1.86
-1-2	36.87	61.79	1.25	99.91	1.95
-1-3	37.25	61.42	1.19	99.86	1.88
570716-3-1	36.70	61.00	1.53	99.23	2.40
-3-2	36.09	60.85	1.60	98.54	2.52

A-5

A. (continued)

	wt. %				FeS mol. %
	S	Mn	Fe	Total	
-3-3	36.49	60.94	1.50	98.93	2.36
570721-2-1	37.00	58.68	4.94	100.62	7.64
-2-2	36.15	58.90	4.88	99.93	7.55
-2-3	37.43	59.49	4.38	101.30	6.75
-2-4	36.16	59.21	5.21	100.58	7.96
-3-1	36.60	59.10	4.27	99.97	6.65
-3-2	36.14	59.11	3.91	99.16	6.11
-3-3	36.92	58.99	4.09	100.00	6.38
570725-1-7	35.81	57.70	5.68	99.19	8.83
-1-8	35.03	57.55	6.18	98.76	9.56
-2-1	37.08	56.46	6.32	99.86	9.92
-2-2	37.37	57.04	5.82	100.23	9.12
-2-3	37.25	57.27	5.90	100.42	9.20
-2-4	37.58	57.21	5.69	100.48	8.91
-2-5	37.01	56.39	6.39	99.79	10.04
-3-1	36.53	56.72	5.62	98.87	8.87
-3-2	36.81	57.44	5.35	99.60	8.39
-3-3	36.74	57.20	5.52	99.46	8.67
-3-4	36.18	58.08	5.49	99.75	8.51
-3-5	36.87	56.89	5.59	99.35	8.81
-4-1	36.66	57.21	5.80	99.67	9.07
-4-2	36.44	57.20	5.67	99.31	8.89
-4-3	36.74	57.01	5.84	99.59	9.16
-4-4	36.85	57.50	5.57	99.92	8.69
-4-5	36.68	57.37	5.91	99.96	9.20
-5-1	37.09	57.83	5.28	100.20	8.24
-5-2	36.67	57.34	5.06	99.07	7.99
-5-3	36.82	57.41	5.31	99.54	8.34
-5-6	37.51	58.09	5.51	101.11	8.53
-6-1	35.86	57.99	5.51	99.36	8.55
-6-2	36.16	57.83	5.50	99.49	8.55
<u>Yamada</u>					
1-1-1	37.45	59.82	3.46	100.73	5.38
-1-3	38.02	60.30	3.62	101.94	5.57
-2-1	37.55	59.07	3.51	100.13	5.53
-2-2	37.36	60.16	3.66	101.18	5.65
-2-3	37.19	60.28	3.17	100.64	4.92
-3-1	37.70	60.43	3.75	101.88	5.76
-3-2	37.69	59.98	3.67	101.34	5.67
-3-3	37.61	59.44	3.74	100.79	5.82
<u>Fukadani</u>					
50122801-1-1-1	37.77	57.28	6.13	101.18	9.52
-1-2-1	37.54	54.70	8.66	100.90	13.47
-1-2-2	37.72	55.28	7.87	100.87	12.29
-1-3-1	37.66	55.92	7.14	100.72	11.16
-1-5-1	37.43	55.07	8.29	100.79	12.89
-3-3-1	37.80	56.47	7.41	101.68	11.43
-3-3-2	37.74	56.77	7.31	101.82	11.24
-4-4-1	37.27	56.91	7.43	101.61	11.38
-4-4-2	37.39	57.45	6.72	101.56	10.31
-4-4-3	37.40	56.81	7.08	101.29	10.91
-5-5-1	37.76	56.82	7.16	101.74	11.03
<u>Fukumaki</u>					
5711516-2-1	37.04	63.58	0.21	100.83	0.32
-3-1	37.31	63.23	0.18	100.72	0.27
-3-2	37.01	63.12	0.26	100.39	0.40

A-6

A. (continued)

	wt. %				FeS mol. %
	S	Mn	Fe	Total	
5711521-1-1	37.74	63.24	0.32	101.30	0.49
-1-2	37.86	63.19	0.33	101.38	0.51
-2-1	37.63	63.05	0.34	101.02	0.52
-2-2	37.80	63.24	0.32	101.36	0.49
-3-1	38.02	63.29	0.33	101.64	0.50
-3-2	37.94	63.27	0.34	101.55	0.52
571121-1-2	36.78	64.20	0.47	101.45	0.72
-2-1	37.32	63.77	0.55	101.64	0.85
-2-2	37.25	63.53	0.53	101.31	0.82
-3-1	37.23	63.53	0.57	101.33	0.88
571193-1-1	37.69	63.49	0.73	101.91	1.13
-1-2	37.49	63.69	0.63	101.81	0.97
-2-2	37.42	63.62	0.56	101.60	0.87
-3-1	37.60	63.68	0.34	101.62	0.51
571145-1-1	37.14	63.28	0.89	101.31	1.37
-1-2	37.30	62.82	0.85	100.97	1.32
-2-1	37.06	63.85	0.63	101.54	0.97
-2-2	37.03	63.03	0.76	100.82	1.17
-3-1	37.20	63.18	0.75	101.13	1.16
-3-2	36.93	63.34	0.63	100.90	0.97
5711524-1-1	37.91	63.14	0.62	101.67	0.96
-1-2	37.82	63.01	0.66	101.49	1.03
-2-1	37.80	62.64	0.68	101.12	1.06
-2-2	38.02	63.02	0.60	101.64	0.93
-3-1	37.73	62.34	0.99	101.06	1.54
-3-2	37.96	62.75	0.75	101.46	1.17
5711109(c)-2-1	37.85	62.87	0.82	101.54	1.27
-2-2	37.52	63.30	0.77	101.59	1.18
-3-1	37.80	62.82	0.79	101.41	1.22
-3-2	37.40	62.65	0.81	100.86	1.26
5711505-1-1	37.33	62.38	1.08	100.79	1.67
-1-2	36.88	62.61	0.80	100.29	1.25
-2-2	37.50	62.60	1.06	101.16	1.64
-3-1	37.37	62.63	0.97	100.97	1.50
-3-2	37.33	62.78	0.96	101.07	1.49
5711109(b)-1-1	37.43	63.30	0.50	101.23	0.77
-2-1	37.77	63.52	0.54	101.83	0.84
-2-2	37.60	63.44	0.57	101.61	0.89
-3-1	37.65	62.64	1.58	101.87	2.42
-3-2	37.72	62.71	1.40	101.83	2.14
-3-3	37.47	62.72	0.96	101.15	1.48
-3-4	37.42	62.92	1.12	101.46	1.72
-3-5	37.31	62.96	1.53	101.80	2.34
571118-1-1	37.31	62.05	1.34	100.70	2.08
-1-2	36.79	62.12	1.42	100.33	2.20
-2-1	37.28	61.97	1.27	100.52	1.97
-2-2	37.03	62.28	1.20	100.51	1.86
-3-1	37.05	62.41	1.15	100.61	1.78
-3-2	37.03	62.78	1.20	101.01	1.85
571154-2-1-1	37.06	61.90	1.41	100.37	2.19
-2-1-2	37.34	61.78	1.32	100.44	2.05
-2-1-3	36.96	62.45	1.37	100.78	2.12
-2-2-1	37.09	61.79	1.35	100.23	2.09
-2-2-2	37.45	61.58	1.23	100.26	1.92
-2-3-1	37.41	61.74	1.22	100.37	1.90
-2-3-2	37.09	61.90	1.29	100.28	2.00

A-7

A. (continued)

	wt. %				FeS mol. %
	S	Mn	Fe	Total	
-2-3-3	37.22	61.68	1.31	100.21	2.05
-1-1-1	36.99	62.30	1.34	100.63	2.06
-1-1-2	37.31	62.16	1.37	100.84	2.11
-1-1-3	37.01	61.94	1.40	100.35	2.16
-1-2-1	37.10	62.40	1.34	100.84	2.07
-1-2-2	37.29	62.14	1.39	100.82	2.14
-1-2-3	37.54	62.55	1.28	101.37	1.97
-1-3-1	37.51	62.17	1.34	101.02	2.08
-1-3-2	37.57	62.39	1.34	101.30	2.06
-1-3-3	37.60	61.70	1.41	100.71	2.20
571148-1-1	37.10	62.11	1.68	100.89	2.59
-1-2	37.23	62.21	1.73	101.17	2.66
-2-1	37.08	62.04	1.77	100.89	2.73
-2-2	37.14	61.91	1.70	100.75	2.63
-3-1	37.09	61.74	1.66	100.49	2.58
-3-2	36.81	61.47	1.66	99.94	2.59
5711109(a)-1-1	37.39	63.39	1.45	102.23	2.20
-2-1	37.59	62.56	2.29	102.44	3.47
-3-1	37.98	63.49	1.39	102.86	2.10
5711128(a)-1-1	37.50	61.66	1.97	101.13	3.05
-1-2	37.30	61.16	2.50	100.96	3.87
-2-1	37.42	61.04	2.07	100.53	3.23
-2-2	37.12	61.23	1.95	100.30	3.04
-3-1	37.55	61.62	2.05	101.22	3.17
-3-2	37.16	61.17	1.96	100.29	3.06
5711515-2-1	37.00	60.51	3.08	100.59	4.77
-2-2	36.82	60.05	3.17	100.04	4.94
-3-1	37.31	59.90	3.48	100.69	5.40
-3-2	37.28	59.89	3.43	100.60	5.33
5711503-1-1	37.49	58.82	4.89	101.20	7.56
-1-2	37.34	58.78	4.45	100.57	6.93
-2-1	37.43	59.28	4.45	101.16	6.87
-2-2	37.26	58.80	4.34	100.40	6.77
-3-1	37.35	59.06	4.58	100.99	7.08
-3-2	37.31	59.35	3.85	100.51	6.00
571159-1-1	37.23	58.90	4.64	100.77	7.20
-1-2	37.28	58.87	4.70	100.85	7.28
-2-1	37.44	58.81	5.33	101.58	8.18
-2-2	37.57	58.57	5.23	101.37	8.07
Kusugi					
58052607-1-2	37.40	58.44	5.95	101.79	9.10
-2-1	37.42	58.31	6.09	101.82	9.31
-2-2	37.47	57.84	6.42	101.73	9.85
-3-1	37.46	56.64	7.60	101.70	11.66
58052602-1-1	37.46	57.47	6.49	101.42	9.99
-1-2	37.39	57.14	7.12	101.65	10.92
-2-1	37.65	57.78	6.05	101.48	9.34
-2-2	37.60	57.91	6.24	101.75	9.58
-4-1	37.67	57.01	6.93	101.61	10.68
-4-2	37.45	57.34	6.57	101.36	10.14
58052601-2-1-1	37.73	56.13	7.25	101.11	11.27
-2-1-2	37.36	57.69	5.98	101.03	9.25
-2-1-3	37.48	56.17	7.41	101.06	11.49
-2-2-1	37.65	55.63	8.42	101.70	12.97
-2-2-2	37.68	55.96	7.69	101.33	11.91
-2-2-3	37.59	55.51	7.92	101.02	12.31

A-8

A. (continued)

	wt. %				FeS mol. %
	S	Mn	Fe	Total	
-2-3-1	37.71	55.84	7.32	100.87	11.42
-2-3-2	37.91	55.65	7.65	101.21	11.91
-2-3-3	37.46	56.65	6.50	100.61	10.14
-1-1-1	37.38	56.69	6.87	100.94	10.65
-1-1-2	37.31	56.16	7.53	101.00	11.65
-1-1-3	37.50	56.04	7.62	101.16	11.80
-1-2-1	37.25	55.64	7.80	100.69	12.12
-1-2-2	37.32	55.59	8.13	101.04	12.57
-1-2-3	37.58	55.80	8.14	101.52	12.55
-1-3-1	36.92	55.36	8.16	100.44	12.66
-1-3-2	37.18	56.78	7.35	101.31	11.29
-1-3-3	37.24	56.47	7.30	101.01	11.28
Tsutsumi					
58052004-1-2-1	37.80	61.21	2.93	101.94	4.51
-1-2-2	37.33	60.96	3.23	101.52	4.95
-1-3-1	37.60	60.27	3.27	101.14	5.06
58052006-1-1	37.18	59.15	4.89	101.22	7.52
-3-1	37.39	60.10	4.42	101.91	6.75
-4-2	37.48	59.69	4.33	101.50	6.66
58052015-1-1	37.18	58.19	6.17	101.54	9.45
-2-2	37.47	59.05	5.41	101.93	8.26
Shimozuru					
1-1-6	37.42	60.02	2.89	100.33	4.53
-1-7	37.34	59.95	2.77	100.06	4.34
-1-8	37.06	59.71	2.85	99.62	4.49
-1-9	37.47	59.32	2.87	99.66	4.55
-1-10	37.40	59.64	2.94	99.98	4.62
-2-6	37.03	59.71	2.85	99.59	4.49
-2-7	36.46	58.92	2.84	98.22	4.53
-2-9	37.10	59.42	2.86	99.38	4.53
-2-10	36.45	59.61	2.93	98.99	4.62
-3-4	37.53	59.98	2.87	100.38	4.50
-3-5	37.00	59.83	2.89	99.72	4.54
-3-6	37.45	59.64	2.65	99.74	4.20

B. Sphalerite analyses

	wt. %					mol. %	
	S	Mn	Fe	Zn	Cd	Total	FeS
Inakuraishi							
R.C.-A-2-A*	33.67	16.05	4.64	46.03		100.39	27.06
-A-2-B*	33.94	16.13	5.12	45.07		100.26	27.33
-A-2-C*	33.15	9.04	5.53	52.77		100.49	15.36
-A-3-A	32.98	10.20	3.71	50.66		97.55	18.08
-A-3-B	33.50	5.16	3.14	60.04		101.84	8.78
-A-3-C	33.37	8.38	2.50	57.80		102.05	14.11
-1-1-1	33.69	7.94	3.14	55.58	0.00	100.35	13.75
-1-1-2*	34.60	16.40	9.84	39.11	0.00	99.95	27.81
-1-1-3*	34.89	9.79	14.48	41.86	0.03	101.05	16.53
-1-3-1*	33.69	9.22	3.88	53.35	0.10	100.24	15.92
-1-3-3*	34.14	7.70	4.68	53.77	0.07	100.36	13.39
-2-2-8*	33.91	10.40	3.14	55.05	0.00	102.50	17.39
-1-1-7	33.34	7.50	2.91	57.06		100.81	12.85
-1-1-9	33.51	9.66	4.13	53.61		100.91	16.44

B. (continued)

	wt. %				Cd	Total	mol. %	
	S	Mn	Fe	Zn			MnS	FeS
-1-1-11*	34.61	17.47	8.76	40.76		101.60	28.96	14.27
-1-1-12*	34.09	14.74	9.64	42.65		101.12	24.54	15.78
-1-1-13*	34.19	16.29	10.34	39.90		100.72	27.15	16.95
-1-1-14*	34.24	15.99	8.84	42.01		101.08	26.66	14.49
-1-1-15*	33.57	6.05	8.06	53.31		100.99	10.29	13.49
-1-1-16*	33.32	5.85	7.63	54.37		101.17	9.91	12.71
-1-1-17*	33.71	8.89	9.64	49.40		101.64	14.84	15.84
-1-1-19*	33.82	6.66	8.49	52.57		101.54	11.25	14.11
-1-1-20*	33.59	6.82	10.18	50.60		101.19	11.50	16.86
-1-5-4	33.72	11.27	3.18	53.61		101.78	18.96	5.25
-1-6-7*	33.89	1.85	13.21	51.84		100.79	3.16	22.25
Yamanaka								
A-1-2-A	33.53	7.06	4.14	56.64		101.37	12.01	6.94
-1-3-A	33.13	7.19	3.61	56.43		100.36	12.36	6.11
-1-3-B	33.52	6.65	3.57	57.57		101.31	11.35	6.01
-2-3-A	32.97	7.02	3.41	54.76		98.16	12.44	5.94
-2-3-B	33.36	7.45	4.23	56.20		101.24	12.66	7.06
Nodatamagawa								
S.Z.-1-2-A	33.49	10.94	3.24	54.19		101.86	18.33	5.34
-2-1-A	32.55	7.59	3.49	56.87		100.50	12.90	5.84
-2-2-A	32.77	7.97	3.89	55.18		99.81	13.70	6.58
-2-3-A	32.06	8.04	3.41	55.39		98.90	13.88	5.78
V.O.-3-2-1	33.25	9.79	14.59	42.13		99.76	16.44	24.10
-3-2-2	33.13	9.03	14.94	41.66		98.76	15.37	25.02
-3-2-3	33.14	9.35	14.35	43.06		99.90	15.68	23.66
-3-2-4	33.13	10.24	13.42	42.78		99.57	17.24	22.22
-3-2-5	33.07	9.17	13.40	43.14		98.78	15.64	22.50
-4-2-1	31.39	2.25	1.80	63.53		98.97	3.92	3.07
-4-2-2	30.91	2.39	2.16	63.97		99.43	4.09	3.64
-4-3-1	31.47	4.67	13.86	47.74		97.74	7.99	23.34
-4-3-2	32.22	4.65	12.78	50.14		99.79	7.84	21.18
-4-3-3	32.24	6.23	16.21	43.70		98.38	10.58	27.07
-4-4-1	32.64	3.05	2.95	61.53		100.17	5.29	5.03
-4-4-2	31.62	2.59	2.36	64.69		101.26	4.36	3.91
-4-4-3	32.15	2.30	1.28	63.27		99.00	4.05	2.22
Hagidaira								
570725-1-11	32.75	7.60	12.24	46.04		98.63	13.03	20.64
-1-12	31.52	8.21	11.87	45.74		97.34	14.07	20.02
Fukadani								
50122801-1-1-a	33.89	14.79	10.27	34.58	8.07	101.60	25.55	17.45
-1-3-a	34.08	10.46	14.02	37.22	5.09	100.87	18.03	23.77
-1-3-b	34.10	10.62	13.84	36.93	4.92	100.41	18.41	23.60
Fukumaki								
571118-1-a	34.11	7.42	1.98	58.09		101.60	12.76	3.34
-1-b	34.28	7.61	1.94	57.86		101.69	13.08	3.28
571148-1-a	33.05	8.07	2.50	55.97		99.59	14.01	4.28
-1-b	33.06	7.19	2.68	56.77		99.70	12.49	4.59
-2-a	33.34	8.54	2.53	56.82		101.23	14.53	4.24
5711503-3-a	34.03	10.37	8.38	47.57		100.35	17.70	14.06
-3-b	34.22	10.43	8.61	47.07		100.33	17.84	14.49
Kusugi								
58052607-1-a	34.51	8.36	12.10	45.09		100.06	14.38	20.46
-1-b	34.36	9.36	12.77	43.85		100.34	15.93	21.38
-1-c	34.32	9.50	12.74	42.73		99.29	16.40	21.63
-2-a	34.73	9.35	13.06	43.18		100.32	15.98	21.97
-2-b	34.68	9.83	13.42	42.74		100.67	16.67	22.40

B. (continued)

	wt. %					mol. %	
	S	Mn	Fe	Zn	Cd	MnS	FeS
-3-a	34.49	9.48	13.39	42.84		100.20	16.16 22.45
-3-b	34.34	9.91	13.58	42.06		99.89	16.90 22.79
58052602-2-a	34.63	9.70	13.51	42.99		100.83	16.40 22.48
58052601-2-1-SA	33.96	7.83	11.76	44.92		98.47	13.70 20.25
-2-1-SB	33.66	8.01	11.71	44.82		98.20	14.01 20.14
-2-1-SC	34.11	8.26	11.91	44.40		98.68	14.43 20.45
Tsutsumi							
58052004-1-1-a	33.62	7.21	5.35	54.93		101.11	12.30 8.97
-1-2-a	33.90	7.89	4.78	54.83		101.40	13.45 8.02
-1-2-b	34.17	8.43	4.70	54.85		102.15	14.25 7.81
-1-3-a	34.14	8.77	5.62	54.18		102.71	14.66 9.24
58052015-1-a	34.45	8.26	10.88	47.10		100.69	14.11 18.28
-2-a	33.85	9.06	9.37	47.85		100.13	15.50 15.76
-3-a	34.25	8.87	10.13	47.34		100.59	15.13 17.00

C. Jacobsite analyses**

	wt. %						
	MnO	Mn ₂ O ₃	FeO	Fe ₂ O ₃	MgO	Al ₂ O ₃	TiO ₂ Total
Hamayokogawa							
5208-2-1-A	33.13	1.47	0.00	59.12	0.09	7.76	0.54 102.11
-2-1-B	32.91	1.86	0.00	60.37	0.14	6.66	0.49 102.43
-2-3-A	32.06	1.86	0.00	56.53	0.23	7.83	0.61 99.12
5205-1-2-A	31.40	1.29	0.00	63.58	0.13	3.44	0.23 100.07
-1-2-B	31.27	1.58	0.00	62.84	0.07	3.49	0.19 99.44
-1-3-A	32.43	1.82	0.00	58.24	0.05	7.84	0.21 100.59
-1-3-B	31.26	2.61	0.00	63.83	0.05	2.01	0.23 99.99
-1-3-C	31.43	2.12	0.00	63.35	0.05	3.10	0.15 100.20
-1-4-A	31.69	2.53	0.00	60.97	0.07	4.59	0.22 100.07
Nodatamagawa							
112-1-1-A	14.41	0.00	16.47	65.59	0.43	2.90	0.16 99.96
-1-1-B	15.18	0.00	15.54	64.99	0.48	3.06	0.21 99.46
-1-2-B	15.43	0.00	15.53	65.21	0.50	3.31	0.21 100.19
-1-3-B	10.96	0.00	18.97	67.55	0.20	0.06	0.00 97.74
-2-1-A	7.05	0.00	24.10	69.55	0.05	0.04	0.02 100.81
-2-2-A	13.39	0.00	16.22	66.41	0.79	1.59	0.11 98.51
-2-3-A	24.90	0.00	4.90	63.47	0.94	3.86	0.29 98.36
-2-3-B	25.40	0.00	4.60	64.03	0.66	3.10	0.29 98.08
Kaso							
28-1-A	40.38	0.72	0.00	42.07	0.72	4.75	10.89 99.53
-2-A	35.39	1.41	0.00	50.31	0.50	8.76	4.05 100.42
-2-B	37.80	0.80	0.00	47.65	0.55	6.84	7.03 100.67
-2-C	35.09	0.92	0.00	51.42	0.37	9.41	3.35 100.56
-3-A	33.74	1.52	0.00	52.58	0.68	10.82	1.90 101.24
-3-B	32.81	2.06	0.00	53.96	0.58	8.45	1.72 99.58
29-2-1-A	34.78	2.03	0.00	50.27	1.76	5.18	5.99 100.01
-2-1-B	32.65	1.26	0.00	53.22	1.45	10.17	2.17 100.92
-2-1-C	34.93	1.90	0.00	49.73	1.83	4.63	6.76 99.78
-2-2-A	36.57	1.97	0.00	50.13	1.18	5.62	6.52 101.99
-2-2-B	33.98	0.30	0.00	52.79	1.10	9.37	3.25 100.79
-2-3-A	39.54	0.11	0.00	43.37	0.94	5.62	10.12 99.70
22-B-2-4-A	35.67	0.00	4.71	44.44	0.07	5.59	9.48 99.96
-2-4-B	37.50	0.00	5.39	39.88	0.11	3.79	12.76 99.43
-2-4-C	33.89	0.00	4.71	48.42	0.07	6.17	7.26 100.52
-2-4-D	34.35	0.00	4.57	46.56	0.04	6.90	7.59 100.01

D. Rhodonite analyses

	wt. %						
	MnO	FeO	MgO	CaO	SiO ₂	Al ₂ O ₃	TiO ₂ Total
Hagidaira							
570719-4-3	45.44	0.22	2.08	6.99	47.15	0.01	0.00 101.89
-4-4	44.98	0.19	2.08	6.84	47.04	0.01	0.01 101.15
-5-3	47.09	0.10	1.26	5.04	46.68	0.01	0.01 100.19
-5-6	47.26	0.09	1.14	5.23	46.43	0.02	0.01 100.18
-6-4	47.69	0.14	1.31	4.58	45.31	0.01	0.00 99.04
570720-1-2	42.53	0.19	3.40	7.08	47.80	0.01	0.00 101.01
570724-1-2	52.32	0.15	0.50	2.57	43.59	0.00	0.01 99.14
-1-5	52.38	0.15	0.44	2.79	44.12	0.00	0.00 99.88
-3-2	54.08	0.19	0.43	1.67	43.20	0.01	0.00 99.58
-3-4	53.62	0.27	0.44	1.71	42.55	0.00	0.00 98.59
-3-5	52.76	0.19	0.54	2.72	43.08	0.02	0.01 99.32
570716-1-2	49.18	0.31	0.33	4.72	45.90	0.01	0.00 100.45
-1-3	49.35	0.52	0.19	4.26	46.27	0.02	0.00 100.61
-2-1	47.70	0.07	0.85	5.48	46.18	0.00	0.00 100.28
-2-2	47.50	0.20	0.73	6.20	45.90	0.01	0.00 100.54
-2-4	48.42	0.17	0.66	5.60	46.12	0.01	0.01 100.99
-2-7	48.43	0.18	0.69	5.49	46.41	0.01	0.00 101.21
-3-2	50.63	0.18	0.65	3.45	45.75	0.01	0.00 100.67
-3-4	50.49	0.17	0.59	4.34	46.14	0.02	0.00 101.75
-3-6	48.70	0.13	0.50	5.60	46.60	0.02	0.01 101.56
570721-1-2	44.08	0.41	0.93	4.49	47.24	0.00	0.01 101.16
-2-1	46.32	4.00	0.71	4.19	45.98	0.01	0.00 101.21
-2-3	46.27	2.88	0.59	4.70	46.20	0.00	0.01 100.65
-2-4	45.46	2.98	0.69	5.19	47.21	0.00	0.01 101.54
-3-2	47.28	2.93	0.61	4.72	45.99	0.00	0.00 101.53
-3-3	45.76	3.53	0.68	4.65	46.48	0.02	0.01 101.33
570725-1-2	48.58	0.44	1.69	3.63	44.06	0.01	0.00 98.41
-2-1	48.83	1.02	1.62	3.34	44.34	0.01	0.00 99.16
-2-3	49.21	0.61	1.87	3.05	45.22	0.00	0.00 99.96
-3-3	48.42	0.42	1.53	4.44	44.76	0.01	0.00 99.58
Fukumaki							
571121-4-4	45.05	0.10	0.68	8.34	44.53	0.01	0.00 98.71
-4-5	45.56	0.12	0.70	7.91	43.71	0.01	0.01 98.02
571145-2-2	49.73	0.13	0.52	4.11	46.02	0.79	0.00 101.30
-2-3	51.04	0.19	0.59	2.99	45.29	0.98	0.00 101.08
-2-4	50.43	0.22	0.45	3.44	45.02	0.49	0.00 100.05
-2-5	50.15	0.24	0.45	3.88	45.03	0.82	0.00 100.57
5711515-2-3	47.72	0.71	2.12	3.73	47.11	0.01	0.00 101.40
-3-2	47.56	0.70	2.03	4.22	46.40	0.00	0.02 100.93
5711503-1-1	50.86	1.44	0.52	2.45	46.11	0.01	0.01 101.40
-1-2	50.60	1.67	0.54	2.47	45.98	0.01	0.02 101.29
-2-1	50.17	1.93	0.54	2.56	46.76	0.00	0.01 101.97
-2-2	50.75	1.21	0.51	2.87	46.47	0.02	0.01 101.84
-3-1	50.91	1.14	0.51	2.66	46.60	0.04	0.01 101.87
-3-5	51.09	1.05	0.52	2.73	46.38	0.00	0.00 101.77
-4-1	49.99	1.15	0.52	3.07	46.65	0.02	0.01 101.41
571159-1-1	50.80	1.13	0.49	2.44	46.12	0.01	0.03 101.02
-1-2	50.18	1.21	0.54	2.56	46.18	0.02	0.01 100.70
-2-2	50.48	1.05	0.51	2.09	44.67	0.01	0.01 98.82
-2-3	50.40	1.04	0.54	2.81	45.77	0.02	0.01 100.59
-2-4	51.51	1.11	0.55	2.13	46.12	0.01	0.00 101.43
Kusugi							
58052607-1-1	50.04	2.90	1.57	0.97	42.87	0.01	0.01 98.37

D. (continued)

	wt. %						
	MnO	FeO	MgO	CaO	SiO ₂	Al ₂ O ₃	TiO ₂ Total
-1-2	47.82	2.74	1.55	3.17	44.18	0.01	0.00 99.47
-2-1	50.59	2.49	1.95	0.38	43.09	0.02	0.00 98.51
-2-2	48.99	3.50	1.97	0.38	44.58	0.01	0.01 99.44
-2-3	49.10	2.79	2.40	0.57	43.63	0.01	0.01 98.51
-3-1	50.53	2.24	1.50	1.26	44.44	0.01	0.01 99.99
-3-2	50.35	2.49	1.49	0.92	44.06	0.01	0.00 99.32

E. Pyroxmangite analyses

	wt. %						
	MnO	FeO	MgO	CaO	SiO ₂	Al ₂ O ₃	TiO ₂ Total
Fukadani							
50122801-1-1	45.85	3.62	3.20	1.78	47.03	0.01	0.00 101.49
-1-2	45.74	4.26	3.73	0.71	46.88	0.01	0.01 101.34
-1-3	43.68	3.52	5.09	1.36	47.77	0.02	0.00 101.44
-2-1	45.87	4.09	3.23	1.22	46.93	0.00	0.01 101.35
-2-2	42.36	8.16	1.99	1.73	46.35	0.01	0.00 100.60
-3-1	45.19	4.69	3.41	0.77	46.38	0.02	0.00 100.46
-3-4	44.64	4.23	4.73	0.93	47.20	0.04	0.00 101.77
Tsutsumi							
58052015-1-1	47.94	0.72	4.16	0.32	47.47	0.09	0.00 100.70
-1-2	48.92	0.74	4.52	0.26	46.74	0.01	0.00 101.19
-1-3	48.54	0.69	4.11	0.50	46.47	0.02	0.00 100.33
-3-1	48.31	0.73	4.61	0.30	46.85	0.02	0.00 100.82
-3-2	49.72	0.74	3.57	0.73	45.87	0.01	0.00 100.64
-5-1	48.49	0.74	4.88	0.38	46.62	0.00	0.01 101.12
-5-2	48.90	0.75	4.63	0.37	46.32	0.02	0.00 100.99

F. Tephroite analyses

	wt. %						
	MnO	FeO	MgO	CaO	SiO ₂	Al ₂ O ₃	TiO ₂ Total
Shōwa							
570709-2-5	66.63	4.74	0.74	0.01	27.94	0.00	0.07 100.13
-3-2	66.58	4.26	0.74	0.02	27.00	0.00	0.32 98.92
-3-5	66.77	3.48	0.89	0.03	27.80	0.01	0.08 99.06
-4-3	65.77	4.79	0.74	0.04	27.13	0.01	0.38 98.86
Hagidaira							
570728-3-2	67.20	0.42	2.99	0.10	28.90	0.01	0.02 99.64
-3-3	67.13	0.39	2.97	0.09	27.99	0.03	0.01 98.61
-3-5	67.28	0.36	3.05	0.08	28.91	0.01	0.00 99.69
570730-1-1	67.13	0.41	3.06	0.11	28.08	0.00	0.01 98.80
-1-3	67.15	0.42	3.03	0.10	28.40	0.00	0.00 99.10
-1-5	67.42	0.39	3.06	0.09	28.23	0.00	0.03 99.22
-2-1	67.85	0.37	3.03	0.09	28.32	0.04	0.03 99.73
-2-2	66.88	0.42	3.06	0.11	28.68	0.01	0.02 99.18
-2-3	66.94	0.41	3.11	0.10	29.05	0.00	0.02 99.63
-2-4	67.26	0.44	3.00	0.11	28.32	0.01	0.00 99.14
-2-5	67.46	0.42	3.15	0.08	28.49	0.01	0.00 99.61
-3-1	67.82	0.41	2.95	0.09	27.15	0.01	0.00 98.43
-3-2	67.84	0.37	2.96	0.14	28.04	0.00	0.01 99.36
-3-3	67.40	0.43	3.10	0.09	28.48	0.01	0.02 99.53

A-13

F. (continued)

	wt. %						
	MnO	FeO	MgO	CaO	SiO ₂	Al ₂ O ₃	TiO ₂ Total
-3-4	67.31	0.43	2.80	0.09	28.10	0.01	0.02 98.76
-3-5	67.40	0.37	3.09	0.11	28.88	0.01	0.01 99.87
570719-1-1	65.14	0.77	4.38	0.14	30.22	0.00	0.02 100.67
-1-2	66.18	0.77	4.36	0.10	29.88	0.01	0.00 101.30
-1-4	65.40	0.72	4.44	0.11	29.70	0.01	0.01 100.39
-2-3	65.94	0.89	4.30	0.14	29.77	0.00	0.01 101.05
-2-5	66.14	0.81	4.43	0.11	29.64	0.01	0.00 101.14
-3-1	68.39	0.83	2.41	0.21	30.10	0.03	0.00 101.97
-3-5	68.44	0.89	2.20	0.25	29.86	0.01	0.00 101.65
-4-1	68.15	0.56	2.50	0.39	30.19	0.00	0.00 101.79
-6-1	67.98	0.73	1.58	0.18	29.12	0.00	0.00 99.59
-6-3	66.96	0.80	2.46	0.10	29.05	0.00	0.00 99.37
570720-1-1	62.98	0.92	6.03	0.24	30.16	0.01	0.00 100.34
-1-3	62.69	0.79	6.91	0.30	29.96	0.00	0.00 100.65
-2-1	61.81	0.79	6.63	0.32	29.31	0.00	0.00 98.86
-2-2	65.79	1.01	4.29	0.02	29.89	0.01	0.00 101.01
-2-3	66.82	0.99	3.02	0.01	29.44	0.00	0.00 100.28
-2-4	66.00	0.98	3.37	0.02	29.78	0.00	0.00 100.15
-2-5	61.71	0.82	7.21	0.34	30.32	0.00	0.00 100.40
570724-1-3	71.25	0.74	0.69	0.11	26.83	0.01	0.00 99.63
-1-4	70.62	0.82	0.74	0.08	27.07	0.00	0.00 99.33
-2-1	71.04	1.10	0.69	0.10	28.05	0.01	0.02 101.01
-2-2	70.42	0.94	0.77	0.10	26.36	0.00	0.00 98.59
-2-3	71.36	0.89	0.71	0.11	27.12	0.00	0.02 100.21
-2-4	70.73	0.73	0.68	0.14	27.35	0.00	0.00 99.63
-2-5	70.73	1.15	0.60	0.12	27.41	0.00	0.00 100.01
Fukumaki							
571121-2-4	69.48	0.69	1.72	0.20	26.92	0.03	0.00 99.04
-2-5	68.59	0.63	1.68	0.18	28.05	0.01	0.02 99.16
-2-6	68.80	0.70	1.70	0.22	28.29	0.03	0.02 99.76
-3-1	68.54	0.53	1.54	0.26	27.54	0.00	0.00 98.41
-3-2	68.70	0.60	1.68	0.26	27.59	0.03	0.00 98.86
-3-3	68.77	0.45	1.55	0.31	26.92	0.00	0.01 98.01
-4-1	68.85	0.36	1.20	0.78	27.14	0.00	0.02 98.35
-4-2	68.88	0.42	1.12	0.93	27.46	0.01	0.01 98.83
-4-3	69.62	0.44	1.30	0.67	27.53	0.03	0.02 99.61
5711109(c)-2-1	70.06	0.93	0.61	0.05	28.40	0.01	0.04 100.10
-2-2	70.17	0.89	0.55	0.04	28.81	0.01	0.02 100.49
-3-1	69.49	0.93	0.56	0.04	28.43	0.03	0.01 99.49
-3-2	70.44	0.87	0.63	0.05	28.87	0.00	0.03 100.89
-4-1	70.40	0.88	0.55	0.06	29.05	0.01	0.02 100.97
-4-2	69.74	0.89	0.52	0.07	28.69	0.03	0.02 99.96
5711505-1-7	66.51	1.20	3.45	0.13	29.34	0.01	0.02 100.66
-1-8	66.30	1.18	3.46	0.12	29.56	0.03	0.02 100.67
-2-5	65.89	1.29	3.36	0.09	29.22	0.00	0.00 99.85
-2-6	66.74	1.26	2.61	0.05	28.99	0.01	0.01 99.67
571118-1-3	68.75	1.53	0.27	0.29	28.80	0.01	0.02 99.67
-1-4	69.83	1.38	0.23	0.28	29.17	0.01	0.00 100.90
-1-5	70.44	1.30	0.22	0.25	29.18	0.01	0.02 101.42
-2-1	70.05	1.27	0.27	0.21	29.23	0.03	0.02 101.08
-2-2	70.52	1.25	0.30	0.19	29.17	0.01	0.01 101.45
-3-3	70.41	1.30	0.23	0.13	29.40	0.03	0.01 101.51
-3-4	70.69	1.27	0.34	0.20	28.71	0.03	0.02 101.26
571148-1-4	69.72	1.47	0.59	0.39	28.81	0.00	0.06 101.04
-1-5	69.51	1.47	0.63	0.39	28.41	0.01	0.02 100.44
-2-3	69.40	1.44	0.55	0.37	27.43	0.01	0.03 99.23

A-14

F. (continued)

	wt. %							
	MnO	FeO	MgO	CaO	SiO ₂	Al ₂ O ₃	TiO ₂	Total
-2-4	69.34	1.66	0.52	0.37	28.27	0.01	0.01	100.18
-2-5	69.90	1.49	0.52	0.36	27.10	0.00	0.02	99.39
-3-3	69.18	1.51	0.59	0.41	28.12	0.03	0.02	99.86
-3-4	69.42	1.55	0.60	0.39	27.03	0.01	0.01	99.01
5711109(a)-1-1	70.33	1.56	0.49	0.11	28.27	0.01	0.01	100.78
-1-2	69.36	1.57	0.55	0.11	28.63	0.03	0.02	100.27
-2-2	69.50	1.62	0.58	0.12	29.12	0.01	0.00	100.95
-2-5	69.37	1.59	0.55	0.13	28.91	0.00	0.01	100.56
-3-2	69.91	1.66	0.52	0.11	28.01	0.03	0.03	100.27
-3-3	70.14	1.61	0.59	0.09	29.13	0.01	0.02	101.59
-3-4	69.51	1.65	0.58	0.13	29.20	0.03	0.02	101.12
-3-5	69.93	1.74	0.55	0.11	28.87	0.01	0.01	101.22
5711128(a)-1-3	62.94	2.43	4.10	0.30	29.98	0.01	0.01	99.77
-1-4	62.87	2.33	4.22	0.29	29.81	0.01	0.01	99.54
-2-3	63.52	2.31	4.07	0.36	29.65	0.01	0.00	99.92
-2-4	63.39	2.24	4.08	0.36	28.99	0.00	0.00	99.06
-3-3	63.24	1.95	4.18	0.45	29.09	0.01	0.00	98.92
-3-4	63.32	1.93	4.10	0.51	29.87	0.01	0.00	99.74
5711515-1-2	65.11	3.08	3.31	0.19	30.24	0.00	0.00	101.93
-3-3	64.70	3.00	3.07	0.20	29.85	0.00	0.00	100.82
-3-4	64.52	3.05	3.15	0.19	29.64	0.00	0.00	100.55
5711503-3-2	65.81	4.68	0.86	0.10	29.57	0.01	0.00	101.03
-3-3	66.09	4.78	0.81	0.08	29.74	0.03	0.00	101.53
571159-2-1	66.48	4.40	0.78	0.14	29.19	0.01	0.02	101.02
Tsutsumi								
58052015-1-4	61.03	4.24	4.30	0.03	30.36	0.01	0.02	99.99
-2-2	61.96	4.02	4.27	0.04	30.24	0.01	0.02	100.56

G. Alleghanyite analyses

	wt. %							
	MnO	FeO	MgO	CaO	SiO ₂	Al ₂ O ₃	TiO ₂	Total
Hanawa								
570733-1-1	66.47	0.22	4.03	0.03	23.06	0.02	0.08	93.91
-1-2	65.97	0.22	3.95	0.02	23.27	0.01	0.04	93.48
-1-4	65.88	0.21	4.22	0.02	23.59	0.13	0.16	94.21
-2-1	65.06	0.23	4.96	0.03	23.98	0.01	0.15	94.42
-2-4	65.35	0.24	4.76	0.02	24.07	0.00	0.06	94.50
-2-5	65.58	0.23	5.28	0.02	23.72	0.03	0.02	94.88
-3-1	66.42	0.22	4.45	0.02	23.72	0.01	0.13	94.97
-3-2	65.97	0.18	4.32	0.01	24.12	0.03	0.12	94.75
-3-4	66.91	0.25	4.40	0.03	23.71	0.01	0.07	95.38
-4-2	66.15	0.20	4.47	0.02	23.87	0.05	0.06	94.82
-4-4	64.85	0.26	4.64	0.01	23.69	0.00	0.15	93.60
Shōwa								
570708-1-2	69.33	0.11	1.08	0.03	23.24	0.03	0.15	93.97
-2-2	69.06	0.14	1.31	0.05	22.54	0.01	0.10	93.21
-3-4	68.89	0.16	1.49	0.05	22.58	0.01	0.15	93.33
570706-1-1	69.01	0.10	2.31	0.04	23.85	0.00	0.15	95.46
-1-2	68.46	0.16	2.28	0.04	23.33	0.00	0.08	94.35
-1-3	68.15	0.16	2.81	0.04	23.73	0.01	0.04	94.94
-2-1	69.01	0.15	2.13	0.02	23.34	0.00	0.06	94.71
-2-2	67.72	0.14	3.28	0.03	24.08	0.01	0.03	95.29
-2-3	68.75	0.18	2.45	0.00	23.53	0.00	0.02	94.93

A-15

G. (continued)

	wt. %							
	MnO	FeO	MgO	CaO	SiO ₂	Al ₂ O ₃	TiO ₂	Total
-2-4	68.65	0.13	2.64	0.04	23.83	0.01	0.05	95.35
-3-1	68.26	0.15	2.62	0.03	22.18	0.03	0.02	93.29
-3-2	68.12	0.17	2.75	0.01	22.71	0.00	0.03	93.79
-3-3	67.96	0.16	3.14	0.03	23.21	0.00	0.03	94.53
-3-4	68.16	0.13	2.58	0.02	23.01	0.01	0.03	93.94
570704-1-1	69.29	0.19	3.27	0.05	25.41	0.00	0.01	98.22
-1-4	70.04	0.16	3.08	0.05	25.09	0.00	0.02	98.44
-1-5	69.71	0.13	3.02	0.04	25.01	0.00	0.04	97.95
-2-1	69.66	0.15	3.65	0.04	25.02	0.00	0.07	98.59
-2-2	69.10	0.18	3.60	0.06	25.35	0.01	0.02	98.32
-2-4	69.33	0.14	3.23	0.04	24.95	0.00	0.03	97.72
-2-5	69.03	0.16	3.68	0.06	24.55	0.00	0.01	97.49
-3-1	68.43	0.09	4.16	0.11	25.14	0.00	0.22	98.15
-3-6	68.13	0.13	3.53	0.04	23.55	0.00	0.28	95.66
570707-1-1	69.67	0.15	1.86	0.06	22.71	0.01	0.08	94.54
-1-4	69.51	0.18	1.85	0.05	23.26	0.00	0.07	94.92
-1-5	68.95	0.19	1.97	0.05	23.23	0.00	0.04	94.43
-2-1	69.14	0.16	1.96	0.06	22.73	0.00	0.01	94.06
-3-1	68.61	0.19	2.22	0.07	22.78	0.01	0.07	93.95
-3-2	69.19	0.18	1.80	0.06	22.50	0.00	0.03	93.76
-3-3	68.10	0.18	2.22	0.05	22.99	0.00	0.08	93.62
Fukumaki								
5711521-1-1	67.93	0.42	2.15	0.04	24.58	0.00	0.33	95.45
-1-2	68.66	0.51	2.23	0.04	24.65	0.03	0.50	96.62
-2-1	68.56	0.48	2.21	0.05	24.46	0.01	0.44	96.21
-2-2	67.96	0.52	2.39	0.05	23.87	0.01	0.43	95.23
-3-1	68.17	0.47	2.32	0.04	24.88	0.01	0.58	96.47
-3-2	67.98	0.52	2.24	0.04	23.98	0.01	0.49	95.26

H. Sonolite analyses

	wt. %							
	MnO	FeO	MgO	CaO	SiO ₂	Al ₂ O ₃	TiO ₂	Total
Shōwa								
570709-1-4	67.41	3.32	1.09	0.06	25.57	0.01	0.41	97.87
-1-5	67.00	3.64	0.96	0.07	24.97	0.10	0.41	97.15
-2-3	68.41	3.19	0.90	0.03	25.06	0.01	0.06	97.66
-2-4	66.66	3.08	0.95	0.03	25.42	0.01	0.34	96.49
-4-1	66.51	3.05	1.04	0.02	24.75	0.03	0.25	95.65
-4-2	66.64	3.15	0.96	0.02	24.65	0.01	0.71	96.14
-4-5	67.24	4.17	0.85	0.12	25.15	0.10	0.26	97.89
Hagidaira								
570728-1-1	67.24	0.29	3.14	0.07	25.55	0.00	0.38	96.67
-1-2	67.20	0.25	3.05	0.08	25.39	0.01	0.18	96.16
-1-3	66.82	0.26	3.16	0.08	25.22	0.01	0.41	95.96
-1-4	65.73	0.30	2.94	0.07	25.13	0.03	0.38	94.58
-1-5	66.66	0.29	3.02	0.09	25.03	0.07	0.18	95.34
-2-1	67.09	0.28	2.86	0.08	24.75	0.00	0.59	95.65
-2-2	66.76	0.29	2.85	0.07	24.94	0.00	0.59	95.50
-2-3	66.90	0.33	2.85	0.06	24.92	0.01	0.59	95.66
-2-4	66.95	0.28	2.85	0.07	25.51	0.00	0.58	96.24
-2-5	67.05	0.28	3.05	0.09	25.52	0.01	0.76	96.76
-3-1	67.73	0.42	3.14	0.08	25.84	0.00	0.03	97.24
-3-4	67.49	0.33	3.11	0.07	25.79	0.01	0.12	96.92

A-16

H. (continued)

	wt. %						
	MnO	FeO	MgO	CaO	SiO ₂	Al ₂ O ₃	TiO ₂ Total
570719-1-3	65.78	0.61	4.57	0.08	27.08	0.03	0.19 98.34
-1-7	66.81	0.52	4.47	0.08	26.84	0.01	0.10 98.83
-2-2	66.06	0.58	4.31	0.04	26.37	0.01	0.13 97.50
-5-1	67.37	0.56	3.01	0.11	26.40	0.00	0.00 97.45
-5-2	66.85	0.51	2.85	0.15	27.23	0.00	0.00 97.59
-5-4	67.34	0.67	1.94	0.01	26.10	0.00	0.00 96.06
-5-5	66.40	0.49	3.14	0.15	26.86	0.00	0.00 97.04
-5-7	65.95	0.53	3.39	0.13	26.81	0.00	0.00 96.81
570720-1-4	57.94	0.61	10.50	0.12	27.49	0.00	0.61 97.27
-1-5	57.71	0.63	9.83	0.42	27.52	0.00	0.96 97.07
<u>Fukumaki</u>							
5711516-1-1	68.88	0.15	1.68	0.05	25.14	0.01	0.42 96.33
-1-2	70.03	0.19	1.71	0.05	26.16	0.03	0.07 98.24
-1-3	69.83	0.21	1.72	0.06	25.75	0.01	0.32 97.90
-2-2	70.87	0.23	1.68	0.05	25.75	0.00	0.07 98.65
-2-3	70.19	0.24	1.62	0.04	25.58	0.00	0.15 97.82
-3-2	68.71	0.20	1.73	0.05	24.72	0.01	0.23 95.65
571121-1-1	67.44	0.51	2.80	0.19	24.91	0.00	0.03 95.88
-1-2	67.56	0.50	2.79	0.19	25.40	0.01	0.02 96.47
-1-3	67.04	0.47	2.90	0.19	25.20	0.01	0.01 95.82
-1-4	68.31	0.45	2.96	0.17	26.28	0.01	0.01 98.19
-2-1	68.20	0.44	2.53	0.21	25.11	0.01	0.01 96.51
-2-2	68.13	0.50	2.30	0.24	25.70	0.00	0.01 96.88
-2-3	68.18	0.51	2.26	0.23	24.67	0.01	0.01 95.87
571193-1-1	68.26	0.52	2.67	0.08	25.71	0.01	0.19 97.44
-1-2	67.45	0.51	2.78	0.08	25.03	0.03	0.43 96.31
-1-3	67.78	0.47	2.70	0.07	25.62	0.01	0.21 96.86
-1-4	67.85	0.55	2.67	0.07	25.21	0.01	0.20 96.56
-1-5	67.21	0.57	2.67	0.09	24.88	0.00	0.43 95.85
571145-1-1	66.94	0.53	3.19	0.06	25.27	0.00	0.37 96.36
-1-2	67.21	0.50	3.14	0.08	26.21	0.00	0.21 97.35
-1-3	67.31	0.55	3.20	0.07	26.26	0.00	0.25 97.64
-1-4	68.05	0.58	3.13	0.06	26.25	0.00	0.04 98.11
-1-5	67.12	0.54	3.16	0.06	26.00	0.00	0.37 97.25
-2-1	67.66	0.55	3.07	0.06	25.92	0.00	0.11 97.37
5711109(c)-1-1	69.69	0.67	0.69	0.07	25.27	0.03	0.56 96.98
-1-2	69.86	0.61	0.52	0.06	25.30	0.03	0.56 96.94
5711505-1-3	64.55	0.86	4.58	0.12	27.14	0.00	0.89 98.14
-1-5	64.80	0.91	4.60	0.13	26.94	0.00	1.01 98.39
-1-6	64.38	0.82	4.45	0.12	26.75	0.00	1.22 97.74
-2-1	64.29	0.87	4.49	0.11	26.61	0.00	1.03 97.40
-2-2	65.39	0.83	4.68	0.10	26.64	0.01	0.74 98.39
-2-8	64.91	0.88	4.63	0.09	26.73	0.00	0.74 97.98

I. Rhodochrosite analyses***

	wt. %				
	MnO	FeO	MgO	CaO	CO ₂ Total
<u>Inakuraishi</u>					
R.C.-2-2-1	55.01	0.18	0.30	4.96	38.46 98.91
-2-2-2	56.42	0.34	0.23	3.34	38.08 98.41
-2-2-3	57.20	0.43	0.27	3.12	38.49 99.51
-2-2-4	56.58	0.24	0.16	3.93	38.51 99.42
-2-2-5	59.77	0.11	0.25	1.88	38.90 100.91

I. (continued)

	wt. %				
	MnO	FeO	MgO	CaO	CO ₂ Total
-2-3-1	60.43	0.44	0.36	0.64	38.66 100.53
-2-3-2	60.03	0.45	0.39	0.62	38.43 99.92
-2-3-3	59.35	0.48	0.38	0.88	38.22 99.31
-2-3-4	61.01	0.17	0.32	0.50	38.70 100.70
-2-3-5	60.57	0.31	0.43	0.87	38.92 101.10
<u>Hanawa</u>					
570733-3-5	58.78	0.12	0.36	2.62	38.99 100.87
-4-5	59.22	0.07	0.38	2.06	38.81 100.54
<u>Shōwa</u>					
570708-1-1	61.77	0.11	0.03	0.56	38.86 101.33
-2-1	60.20	0.08	0.00	0.47	37.77 98.52
-2-3	59.34	0.09	0.00	1.15	37.77 98.35
-2-4	60.11	0.08	0.02	0.72	37.93 98.86
-3-1	59.86	0.10	0.11	0.98	38.09 99.14
570706-1-4	61.40	0.10	0.30	0.69	39.02 101.51
-1-5	59.35	0.12	0.39	0.91	38.03 98.80
-2-5	59.37	0.09	0.31	1.40	38.33 99.50
-3-5	57.65	0.12	0.55	2.82	38.65 99.79
570704-1-2	62.05	0.13	0.05	0.03	38.65 100.91
-3-2	55.23	0.11	0.39	5.80	39.31 100.84
-3-3	52.52	0.07	0.48	7.58	39.10 99.75
-3-4	61.56	0.10	0.00	0.48	38.63 100.77
-3-5	61.74	0.10	0.03	0.00	38.40 100.27
570707-1-2	61.97	0.13	0.14	0.19	38.83 101.26
-2-3	61.00	0.18	0.19	0.80	38.79 100.96
-2-4	61.46	0.11	0.05	0.40	38.57 100.59
-3-4	59.07	0.14	0.28	2.57	39.06 101.12
-3-6	61.89	0.18	0.24	0.23	38.95 101.49
570709-2-1	57.49	0.81	0.58	3.08	39.21 101.17
-2-2	56.15	0.59	0.55	3.45	38.51 99.25
-3-1	57.36	0.56	0.50	3.07	38.88 100.37
-3-4	56.08	0.31	0.64	4.63	39.31 100.97
-4-4	56.54	0.18	1.01	4.16	39.56 101.45
<u>Hijikuzu</u>					
621095-1-1-3	60.88	0.09	0.00	0.76	38.42 100.15
-1-3-2	59.59	0.07	0.00	1.00	37.80 98.46
-1-4-5	58.36	0.13	0.00	2.31	38.10 98.90
<u>Hagidaira</u>					
570730-1-2	33.50	0.06	1.22	24.18	41.13 100.09
-1-4	32.39	0.07	1.45	25.00	41.34 100.25
570719-1-6	36.71	0.10	1.98	19.41	40.23 98.43
570720-3-1	52.23	0.16	4.70	2.22	39.38 98.69
570724-3-3	51.15	1.38	1.38	7.31	39.82 101.04
570716-1-4	53.75	0.29	0.85	5.68	38.91 99.48
-1-5	52.95	0.30	0.85	6.55	39.10 99.75
-2-3	50.43	0.30	0.86	8.06	38.74 98.39
-2-6	50.69	0.25	0.86	8.74	39.40 99.94
-3-1	49.80	0.28	0.34	9.98	39.27 99.67
-3-3	52.61	0.31	0.29	8.31	39.67 101.19
570721-1-1	49.41	2.05	1.14	7.70	39.20 99.50
-1-4	48.47	2.16	1.09	8.37	39.15 99.24
-1-5	48.82	2.06	1.06	8.12	39.08 99.14
-3-4	50.98	1.38	1.23	7.31	39.55 100.45
-3-5	54.77	1.17	1.09	4.95	39.77 101.75
570725-1-4	50.44	2.60	1.82	6.37	39.87 101.10
-2-4	57.57	1.14	0.16	3.24	39.13 101.24

I. (continued)

	wt. %				
	MnO	FeO	MgO	CaO	CO ₂
-3-1	57.88	1.06	1.00	1.55	38.87
Fukadani					
50122801-2-5	50.81	4.12	2.54	3.42	39.50
Fukumaki					
5711516-2-1	55.92	0.11	1.37	4.06	39.44
-3-1	55.80	0.12	1.44	4.60	39.87
-3-3	55.65	0.09	1.24	4.30	39.31
-3-4	61.82	0.10	0.00	0.57	38.86
5711521-1-4	55.46	0.09	1.74	3.77	39.32
-1-5	61.82	0.10	0.03	0.30	38.68
-2-4	61.28	0.11	0.09	0.81	38.82
-3-4	56.50	0.16	1.49	3.36	39.41
-3-5	61.62	0.12	0.05	0.51	38.76
571121-2-7	51.99	0.11	0.28	8.59	39.37
571193-1-7	59.96	0.22	0.19	1.09	38.40
-1-9	60.15	0.31	0.13	0.83	38.30
-1-10	59.67	0.61	0.22	0.88	38.32
-1-11	59.66	0.19	0.16	0.59	37.77
571145-2-8	59.93	0.20	0.11	1.63	38.70
5711109 (c)-3-3	61.68	0.24	0.03	0.47	38.82
-4-4	61.73	0.20	0.00	0.11	38.51
5711505-1-1	31.97	0.13	1.29	25.25	41.14
-1-2	32.48	0.14	1.32	25.29	41.52
-1-4	30.91	0.10	1.22	26.73	41.55
-2-4	39.68	0.13	1.62	16.98	39.79
571118-2-7	47.24	0.14	0.06	12.36	39.16
-3-5	48.91	0.18	0.08	11.68	39.71
-3-6	48.03	0.15	0.05	11.88	39.27
571148-3-5	56.82	0.12	0.08	4.80	39.18
571159-1-5	56.14	0.12	0.64	3.81	38.59
-1-8	56.92	0.16	1.46	3.50	39.75
Tsutsumi					
58052015-3-3	53.34	0.49	4.51	1.01	39.11

* : showing wurtzite-like optical properties.

** : The data were calculated assuming mineral stoichiometry and a perfect electron microprobe analysis.

*** : The data were reduced with the fixed stoichiometry mode with C=Mn+Ca+Mg+Fe.

Appendix II.

Atago	愛宕	Nakanoyama	中野山
Dainichizawa	大日沢	Namiita	浪板方
Fukadani	深谷	Nishikata	西田方
Fukumaki	福巻	Nodatamagawa	野田玉川
Furujuku	古宿	Nomine	野峯
Furumiya	古宮	Ōe	大伊江
Hagidaira	萩平	Ōidani	大伊谷
Hamayokogawa	浜横川	Ōishi	大石
Hanawa	花輪	Ōmori	大盛
Hata	畑	Ritō	利東
Hazu	幡豆	Sankei	三惠
Hijikuzu	肘葛	Sanyō	三陽
Hokkōji	発光路	Shimozuru	下鶴
Hongō	本郷	Shōwa	昭和
Inakuraishi	稲倉石	Taguchi	田口
Ioi	五百井	Takahira	高平
Iwato	岩戸	Takamatsu	高松
Jūniyashima	十二八洲	Takanosu	鷹ノ巢
Kaso	加蘇	Takashima	高島
Kinkō	錦光	Taki	滝
Konakayama	小中山	Tamamori	玉盛
Kuranosawa	倉の沢	Tennō	天尾
Kuratani	久良谷	Toyoka	豊稼
Kurosakaishi	黒坂石	Tsutsumi	堤
Kurumazawa	車沢	Wagi	和木
Kusugi	久杉	Yaei	弥栄
Kyūrasawa	久良沢	Yagisawa	八木沢
Mitsune	三水根	Yakumo	山雲
Mizutani	水谷	Yamada	山田
Mogurazawa	茂倉沢	Yamanaka	山岳
Mori	森	Yūbaridake	夕張岳